

# **FLOOD MAPPING AND WATER LEVEL ESTIMATION USING MULTI-TEMPORAL SENTINEL-1 SAR IN THE PROVINCE OF OVERIJSEL, THE NETHERLANDS**

FIRAOL BEFEKADU GELETA  
February, 2018

SUPERVISORS:

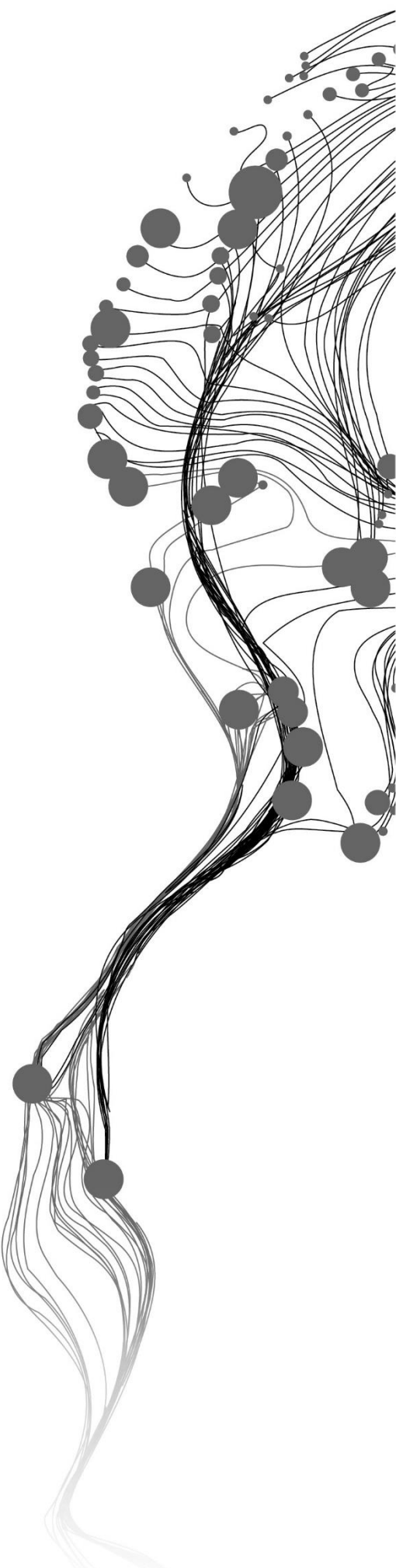
Dr. ir. R. van der Velde

Ir. G.N. Parodi

ADVISOR:

Ir. H.F. Benninga





# **FLOOD MAPPING AND WATER LEVEL ESTIMATION USING MULTI-TEMPORAL SENTINEL-1 SAR IN THE PROVINCE OF OVERIJSEL, THE NETHERLANDS**

**FIRAOL BEFEKADU GELETA**

Enschede, The Netherlands, February, 2018

Thesis submitted to the Faculty of Geo-Information Science and Earth Observation of the University of Twente in partial fulfilment of the requirements for the degree of Master of Science in Geo-information Science and Earth Observation.

Specialization: Water Resources and Environmental Management

**SUPERVISORS:**

Dr. ir. R. van der Velde

Ir. G.N. Parodi

**ADVISOR:**

Ir. H.F. Benninga

**THESIS ASSESSMENT BOARD:**

Dr. ir. C.M.M. Mannaerts (Chair)

Ir. S. Monicxs (External Examiner, Waterboard Vechtstromen, The Netherlands)

Dr. Z. Vekerdy (Department of Water Resources, ITC, University of Twente)

#### DISCLAIMER

This document describes work undertaken as part of a programme of study at the Faculty of Geo-Information Science and Earth Observation of the University of Twente. All views and opinions expressed therein remain the sole responsibility of the author, and do not necessarily represent those of the Faculty.

## ABSTRACT

The increasing availability of remote sensing products with high spatial and temporal resolutions offers the opportunity to retrieve high-quality flood extent maps for monitoring of surface water dynamics. The data obtained from the recently launched Sentinel-1 satellite become an essential information source for the water resources managers, planners, and decision-makers. The capability of images acquiring independent of day/night and all weather conditions make the synthetic aperture radar (SAR) sensors preferable over optical sensors for flood monitoring. In this study, the capability of multi-temporal Sentinel-1 SAR images is explored for the flood extents mapping and the estimation of water levels over the period from October 2014 to March 2017. This has been done for five retention reservoirs and the upper reach of the Dinkel river in the province of Overijssel, the Netherlands.

The analysis in this report showed that the VV polarization achieves the better demarcation of water and land surfaces. SAR images are commonly affected by speckle noise. In this study, this effect was reduced by using Refined Lee speckle filter. The identification of flooded and non-flooded pixels was performed through a thresholding technique. From the multi-temporal images analysis, it is realized that not one single threshold value works efficiently to extract flood extent for all images. This is because of the change in incidence angles due to the different satellite pass and also some environmental conditions. Therefore, the threshold values within certain intervals were applied. According to the flood extent assessment, Dinkel river experienced at it is a peak on February 24, 2016, and flooded area of 131 hectares. Among the others retention reservoirs, the OV0002 reservoir was also filled to its full capacity on February 12, 2016. The others retention reservoirs were observed flooded maximum up to 40 % of their total area.

The estimated water levels from the combination of flood maps and digital elevation model were validated with in-situ measured water levels. For the most of retention reservoirs, the position of water level measurement and where flood was detected did not match. Hence, it was a big challenge for validation of retention reservoirs water levels. In the case of Dinkel river, only a few stations face such problem. The result showed that the best agreement between Sentinel-1 and in-situ measured water levels was obtained for Dinkel river at Bossinkbrug station. At this station, the coefficient of determination ( $R^2$ ) of 0.80 and root mean square error (RMSE) of 16 cm was obtained. For the other stations,  $R^2$  varies from 0.60 to 0.79 and RMSE varies from 18 cm to 27 cm. For the retention reservoirs,  $R^2$  varies from 0.13 to 0.68 and RMSE varies from 34 cm up to 101 cm. Finally, the flood extent maps were developed to provide the information about which locations are frequently flooded. Therefore, water managers can use this information for their management practices. They may create alternative ways of the flood mitigation measures based on their management point of views using this spatial and temporal information of the flood extents obtained from this study.

**Keywords:** Sentinel-1, Synthetic Aperture Radar (SAR), Flood mapping, DEM, Water level estimation

## ACKNOWLEDGEMENTS

First and foremost, I would like to thank God Almighty for His grace, guidance, support, and showering of His blessing throughout my life, and for He sustain me to complete my dissertation.

My special thanks go to Dutch Ministry of Foreign Affairs, for providing me NFP scholarship to pursue my master's study at the faculty of ITC, University of Twente, the Netherlands.

I would like to express my deepest & sincere gratitude to my first supervisor Dr. ir. Rogier. van der Velde, for his invaluable continuous advice, suggestions, and guidance throughout my thesis. I have been lucky to have him as my supervisor who cares about my every work. I would also like to present my sincere appreciation and gratitude for my second supervisor Ir. G.N. Parodi, for his advice and helps. His office door was open for me at any time I face difficulty in my progress. I am also extremely grateful for my advisor Ir. H.F. Benninga, for his guidance, advice, encouragement and for all important information and data he provides me during my study.

I wish to take this opportunity also to thanks Dutch regional water board of *Waterschap Drents Overijsselse Delta* and *Waterschap Vechtstromen*, for providing me necessary data for my research.

I would like to thank all WREM staff and my fellow students at ITC, for their support and friendship, in particular, \*Becky. My special thanks go to my former best teacher Dr. Abebe D. Chukalla. He has been there providing me his heartfelt advice, guidance and inspiration all the time, I say thank you too much. I am also pleased to thanks Mr. Yakob Mohammed, Mrs. Biftu Kebede+D.K., and Mr. Dinkbeyesus Yacob, for their friendship and encouragement extended to me.

Last but not least, I wish to express my heartfelt gratitude to my parents, Tg.+Dani E., Maria B., and Akawak B., for their encouragement, inspiration, and motivation throughout all my study. You are all my spur to this success. I don't have enough word to say; only I say thank you!

*"All Dedicated to Mom rest in peace"*

# TABLE OF CONTENTS

---

1.	Introduction.....	1
1.1.	Background.....	1
1.2.	Research Problem.....	2
1.3.	Research Objective.....	2
1.4.	Thesis organization outline.....	3
2.	Literature Review.....	4
2.1.	Basic principles of SAR imaging.....	4
2.2.	Sentinel-1 SAR mission.....	5
2.3.	Flood mapping from SAR imagery.....	6
2.4.	Water level estimation from remote sensing.....	8
3.	Study Areas and Data Sets.....	9
3.1.	Study Areas.....	9
3.2.	Data Sets.....	11
3.2.1.	Multi-temporal Sentinel 1 SAR Images.....	11
3.2.2.	Digital Elevation Model.....	11
3.2.3.	Water Levels Measurements.....	14
3.2.4.	Rainfall measurements.....	14
4.	Sentinel-1 SAR Pre-processing and Methods.....	16
4.1.	Sentinel-1 SAR pre-processing.....	17
4.1.1.	Range-Doppler Terrain Correction.....	17
4.1.2.	Speckle Filtering.....	17
4.1.3.	Subsetting and Mosaicking.....	19
4.2.	SNAP graph builder.....	19
5.	Open Water Detection.....	20
5.1.	Water surface backscattering mechanisms.....	20
5.2.	Sentinel-1 SAR polarization.....	21
5.3.	SAR-based flood extent extraction technique.....	21
5.4.	Sentinel-1 SAR flood maps.....	24
5.4.1.	Dinkel river time series flood maps.....	24
5.4.2.	Retention reservoirs time series flood maps.....	27
5.5.	Flood frequency maps.....	30
5.5.1.	Dinkel river.....	30
5.5.2.	Retention reservoirs.....	30
5.6.	Water level estimation from flood maps and digital elevation model.....	33
5.7.	Flood extent vs. in-situ measured water levels.....	34
5.8.	Sentinel-1 derived water levels vs. in-situ measured water levels.....	37
6.	Conclusion.....	42
7.	Limitations and Recommendations.....	43
7.1.	Limitations.....	43
7.2.	Recommendations.....	44
	List of references.....	45
	Appendices.....	48

# LIST OF FIGURES

---

Figure 1: Imaging geometry of a side-looking radar system (Source: <a href="http://slideplayer.com/slide/5932621/">http://slideplayer.com/slide/5932621/</a> ) .....	4
Figure 2: Artistic view of Sentinel-1 on the orbit scanning the earth surface (Source: <a href="https://scihub.copernicus.eu/">https://scihub.copernicus.eu/</a> ).....	6
Figure 3: Study area maps: retention reservoirs (upper right, 1) and Dinkel river (lower right, 2) with the background image of Sentinel-2A acquired on May 08, 2016 (available from online map) .....	9
Figure 4: DEM for Dinkel study area mosaicked from six AHN2 DEM tiles. ....	12
Figure 5: DEM for retention reservoirs mosaicked from twenty-eight AHN2 DEM tiles and shows the locations of each retention reservoirs with their elevation.....	13
Figure 6: Water levels and rainfall data were taken for the 2015 year over (a) retention reservoir OK0302 and (b) Dinkel river at Bossinkbrug.....	15
Figure 7: Flowchart of the research methodology used for performing flood mapping and water level estimation from multi-temporal Sentinel-1 SAR images .....	16
Figure 8: Speckle filtering test for image taken on December 22, 2014, near to OV0002 retention reservoir, (A) Terrain image (B) Boxcar (C) Median (D) Frost (E) Gamma-MAP (F) Lee (G) Refined Lee and (H) Lee-Sigma.....	18
Figure 9: Sentinel-1 SAR Batch processing orders on SNAP graph builder. ....	19
Figure 10: Backscattering mechanisms over water and different surface condition. Specular reflection over the water body is shown as very low backscatter (Source: Martinis S., 2010) .....	20
Figure 11: Comparison of VH polarization (a) and VV polarization (b) for the images taken on February 24, 2016, over Dinkel catchment (red circle indicates permanent water, lakes).....	23
Figure 12: The flood maps for Dinkel river shows approximately some low, medium and high flood with the background image of Sentinel-2A acquired on May 08, 2016 (available from online map).....	25
Figure 13: Photograph of the Dinkel flood captured on February 24, 2017, near to the Losser city (source: <a href="https://www.youtube.com/watch?v=fdCfSIzsd04">https://www.youtube.com/watch?v=fdCfSIzsd04</a> ).....	26
Figure 14: Number of the time-series Sentinel-1 SAR images observed as the flood for each month of the year starting from October 2014 to March 2017, to indicate which months are usually flooded.....	26
Figure 15: OV0002 retention reservoir time series flood map (November 08, 2014 to March 26, 2017). The place observed as a flood for every image is the part of Vecht river, and the yellow line indicates the location of OV0002 retention reservoir .....	28
Figure 16: DV0277 retention reservoir time series flood map (November 28, 2014, to March 2, 2017).....	29
Figure 17: Flood frequency map for Dinkel river developed from the combination of flood maps between December 14, 2014, and March 11, 2017.....	31
Figure 18: Flood frequency maps developed for retention reservoirs from the flood maps between October 08, 2014 to March 26, 2017 .....	32
Figure 19: Water level estimation from flood map (February 10, 2016) merged with DEM for Dinkel river .....	33
Figure 20: Comparison of flood surface area with in-situ measured water lever for Dinkel river.....	35
Figure 21: Comparison of flood surface area with in-situ measured water lever for retention reservoirs ...	37
Figure 22: Correlation results between Sentinel-1 derived and in-situ measured water lever for Dinkel river .....	38
Figure 23: Correlation results between Sentinel-1 derived and in-situ measured water lever for retention reservoirs.....	40

## LIST OF TABLES

---

Table 1: Satellite missions featuring SAR systems (Source: Grimaldi et al., 2016) .....	5
Table 2: Spatial characteristics of Sentinel-1 acquisition modes (Source: Sentinel-1 user handbook).....	6
Table 3: Retention reservoirs characteristics.....	10
Table 4: The main characteristics of Sentinel-1 Interferometric Wide swath mode (Source: Sentinel-1 user-guide) .....	11
Table 5: Summary of performance assessment for both study areas.....	41

## LIST OF ABBREVIATIONS

---

AHN2	<i>Actueel Hoogtebestand Nederland -2</i> (current Altitude File Netherlands - 2)
DEM	Digital Elevation Model
DLR	<i>Deutsches Zentrum für Luft- und Raumfahrt</i> (German Aerospace Center)
ENVI	Environment for Visualizing Images
ENVISAT	Environmental Satellite
ERS-1/2	European Remote Sensing - 1/2
ESA	European Space Agency
EW	Extra Wide swath mode
GIS	Geographic Information System
GRD	Ground Range Detected
IDL	Interactive Data Language
InSAR	Interferometric Synthetic Aperture Radar
IW	Interferometric Wide Swath
KNMI	<i>Koninklijke Nederlands Meteorologisch Instituut</i> (Royal Netherlands Meteorological Institute)
PDOK	<i>Publieke Dienstverlening op de Kaart</i> (Public Services On the Map)
R <sup>2</sup>	Coefficient of determination
RMSE	Root Mean Square Error
S1	Sentinel-1
SAR	Synthetic Aperture Radar
SLC	Single Look Complex
SM	Strip map Mode
SNAP	Sentinel Application Platform
WDODelta	<i>Waterschap Drents Overijsselse Delta</i>
WM	Wave Mode

# 1. INTRODUCTION

## 1.1. Background

Floods are categorized among the most frequently occurring natural hazards in the world and have far-reaching effects on human lives and environment. The Netherlands is among a country highly vulnerable to the effects of the floods (Jongman et al., 2014). This country is situated in a low-land delta and historically characterized by its *“fight against water”* (Kaufmann et al., 2016). Flooding usually occurs due to riverine flooding and sometimes also due to increase in sea water level. Currently, considerable attention is given to flood controls aspects by national and regional water authorities. The development of flood extent maps is a very crucial issue for flood controlling and its management. Flood maps provide a more direct and strong impression than other ways of presentation of the floods (Erlach et al., 2007). Flood maps represent the spatial distribution of flooding situations. Furthermore, flood maps are essential for the development of flood management strategies likes flood risk maps (Twele et al., 2016). During the past years, flood maps are developed using geographic information systems (GIS) and hydraulic models (Demir & Kisi, 2016). Recently, flood extent mapping from space is becoming more and more recognized as an approach to providing information to planners, decision-makers and water resources managers (Manjusree et al., 2012). Satellite images are advantageous over in-situ water level measurements because of the ability to cover large spatial extents in a timely fashion (Clement et al., 2017). In addition, flood extents and water levels data retrieved from remote sensing are of benefit for ungauged river basins.

Nowadays various remote sensing products are available. Synthetic Aperture Radar (SAR) products are considered as particularly appropriate for flood monitoring. Compared to the other sensors, SARs provide data of the earth surface independent of weather conditions and at day and night time (Chini et al., 2016). Also, SARs are capable of acquiring high-resolution microwave observations that make them suitable for local applications such as flood extent mapping. An improved revisit frequency and spatial coverage (Potin, 2013) of SAR products through the launch of a Sentinel-1 satellite by European Space Agency (ESA), Sentinel-1A and 1B on 3rd April 2014 and 22nd April 2016, respectively increase the utilization of SAR products for surface water detection. The Sentinel-1A and 1B SAR sensors have a better spatial-temporal resolution than the previous ESA satellites such as ERS-1/2. The freely available Sentinel-1 data make them interesting for operational applications.

The C-band (5.405 GHz) SAR system mounted onboard of the Sentinel-1 satellites transmits a radar pulse and records the radiation scattered in the backward direction (Clement et al., 2017). The amount of the radiation returned back depends on the factors like dielectric and geometric properties of the target as well as sensing configuration such as polarization, wavelength and incidence angles (Gan et al., 2012). Water bodies return low backscatters because a large amount of radiation is specularly reflected away from the sensor as open water surfaces are typically smooth (Schlaffer et al., 2015). The detection of open water using SAR sensors is complicated by water surface roughening caused by wind, rain or vegetation (Alsdorf et al., 2007). Image acquisition mode (polarizations) based on the geometric plane that radar transmitted and received signals are needed to be considered when acquiring the images since they have a significant effect on the detection of floods. There are a number of algorithms are available for the extraction of water bodies from satellite images including histogram thresholding (Henry et al., 2006; Brown et al., 2016), fuzzy classification (Martinis et al., 2015; Twele et al., 2016), texture analysis (Pradhan et al., 2014) and region growing (Matgen et al., 2011; Martinis et al., 2015).

Flood extent maps allow an estimation of spatially distributed water levels (Giustarini et al., 2011). Usually, river and reservoir water levels are monitored through extensive fieldwork using measurement gauging (Barreto et al., 2016). However, the current availability of high spatial and temporal resolution of SAR images allows monitoring of surface water extent from space. There are different ways to deduce water levels from the flood extent captured by SAR. One of these methods is combining the flood extent maps with a digital elevation model (DEM), which is called an indirect method (Hostache et al., 2009; Giustarini et al., 2011; Grimaldi et al., 2016). An indirect method of water level may work in particular for an area having high-resolution DEM like the Netherlands.

In most of the previous studies, only one or few images were used for flood extent mapping (Tsyganskaya et al., 2016). However, it is not possible to show the temporal variations of surface water by having only single images. Therefore, multiple images are required to show the temporal variations of the flood extent. The availability of multi-temporal images facilitates understanding, quantifying and monitoring of surface water for improved water resource management from the space (Santoro & Wegmüller, 2014). This study aims to use Sentinel-1 multi-temporal images for the generation of time series of flood extent maps, use in-situ measured water levels to verify the mapped flood extents and investigate the potential of estimating water levels from the SAR images.

## **1.2. Research Problem**

Two-thirds of the Netherlands is prone to the floods. A large part of the country is suffering from potential riverine flooding. This happens due to its lowland features, and some major transboundary rivers flowing towards the Netherlands. To secure the water safety for the population and protect the environment, an intensive flood control approach with effective management is important. This could be possibly achieved by having maps showing the spatial distribution of flood extents, which can be obtained possibly from the remote sensing imageries, such as Sentinel-1.

The regional water management authority Waterschap Drents Overijsselse Delta (WDODelta) has a keen interest in the mitigation of the floods. They have created flood retention reservoirs to store surface water in times of water excess to delay the discharge towards the lower areas and release more gradually in the hope to increase the flood resilience downstream. So, they are interested in learning whether the retention reservoirs work as they are supposed to do. In the management area of the regional water management authority of Waterschap Vechtstromen, farmers are financially compensated for flooding along the Dinkel river. So, both the operational water managers as well as the farmers are interested in learning which lands along the Dinkel flooded and whether this is according their agreement.

## **1.3. Research Objective**

### **1.3.1. General Objective**

The main objective of this research is to generate flood extent maps and estimate the water levels using multi-temporal Sentinel-1 SAR images for selected retention reservoirs, and the upper reach of the Dinkel river.

### **1.3.2. Specific Objectives and research questions**

The following specific objectives are formulated for achieving the main objective:

- i. Develop a method for delineating flood extents using Sentinel-1 images acquired over flood retention reservoirs of different size and along the upper reach of the Dinkel river,

- ii. Quantify the water levels through combination of the flood extent maps with a high-resolution DEM,
- iii. Verify the reliability of the flood extent maps through comparison of water levels estimated from Sentinel-1 images and measured in-situ by the responsible regional water authorities.

The following research questions are defined:

- i. Which type of floods delineation method is most suitable for generation of multi-temporal flood extent maps?
- ii. Which technique of water level estimation is most suitable for quantifying water levels from remote sensing imagery over the study areas?
- iii. Is it possible to verify the reliability of flood extent maps through comparison of water levels measured in-situ and water levels derived from Sentinel-1 (S1) with the combination of a high-resolution DEM?

#### **1.4. Thesis organization outline**

This thesis is organized into seven chapters. Chapter two presents a literature review explaining the basic principles of SAR, SAR based flood mapping and water level estimation. Chapter three describes the study area and the data used like multi-temporal Sentinel-1 SAR images, AHN2 digital elevation model, in-situ water levels measurement and rainfall data. Chapter four describes the methods and the pre-processing of the Sentinel-1 SAR images. Chapter five encompasses the selection of Sentinel-1 SAR polarization, and the approach of flood extent extraction was used for this study. Results and discussion of the flood maps and water level estimations also included in this section. Chapter six gives the conclusion based on the finding of the research. Finally, chapter seven outlines the limitations and recommendations of this study.

## 2. LITERATURE REVIEW

### 2.1. Basic principles of SAR imaging

Following the history of the SAR, the concept and applications of SAR have grown over time since 1950 after Carl Wiley (McCandless & Jackson, 2004). Carly Wiley, of the Goodyear Aircraft Corporation, invented the use of Doppler frequency analysis of reflected signals from a moving coherent radar to improve along-track width (Zyl & Kim, 2011). Since this time, several studies have been performed that contributed to the current technological development of airborne and spaceborne SAR missions. A technological advancement over microwave sensors has been tremendously increased since the first launch of SEASAT, which was the first civilian spaceborne SAR satellite in June 1978 (McCandless & Jackson, 2004; Torres et al., 2012). However, the policy for the availability of the data to public services is not the same for all sensors. Most of them are commercial or need a special request, and only some of them are allowed for public use.

Basically, SARs are side-looking radar systems taking the images from multiple observations by moving along its orbital path to enable construction of high-resolution images. They transmit electromagnetic signals that interact with the surface of the objects and records the backscattered echoes by the radar antenna in a sequential manner (DLR, 2013). The amount of the backscattered signals that returns back to the sensor are a function of some specific properties of SAR systems (Gan et al., 2012). These properties may classify as system specific properties like incidence angle, wavelength, polarization and object specific properties like surface roughness and dielectric properties of the surface. SAR systems are capable of generating a high-resolution image by means of combining coherently received echoes that enable the development of a virtual aperture that is more longer than the physical antenna length (DLR, 2013; radartutorial.eu, 2017). Figure 1 provides the overview of imaging SAR geometry. Resolution in range and azimuth direction is characterized a SAR system. The higher resolution in range direction is possible due to short pulse return duration while the azimuthal resolution depends on the antenna length and is independent of orbit height (Martinis, 2010).

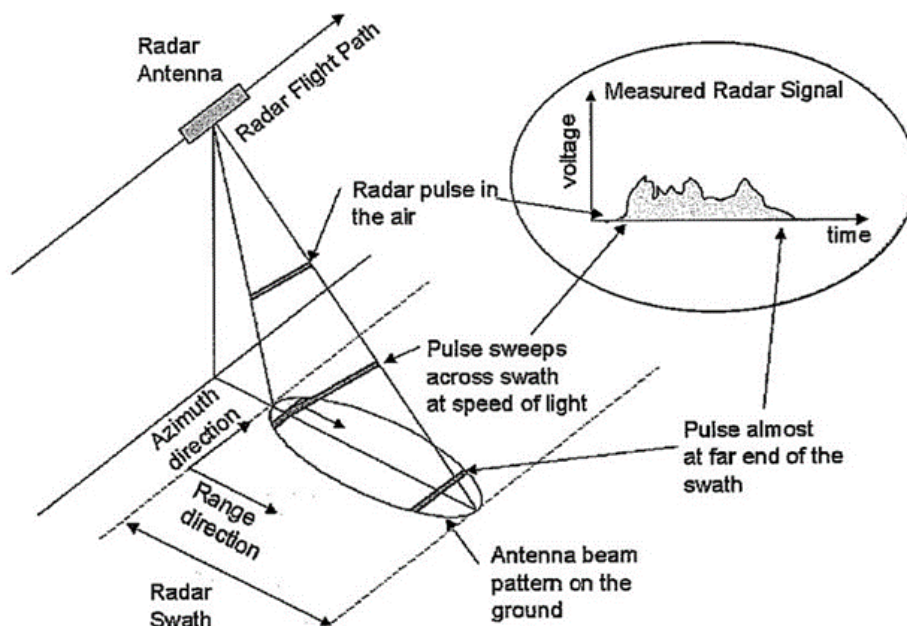


Figure 1: Imaging geometry of a side-looking radar system (Source: <http://slideplayer.com/slide/5932621/>)

## 2.2. Sentinel-1 SAR mission

Sentinel-1 SAR is the first operational SAR satellite comprising of two polar-orbiting satellites, Sentinel-1A and 1B launched on 3rd April 2014 and 22nd April 2016, respectively (Potin, 2013). It is designed for seven years lifetime with consumables for 12 years. Sentinel-1 is a satellite project that is financially supported by the European Union and carried out under Copernicus programme. Its data is open and freely available to the public. Sentinel-1 operates at C-band (5.405 GHz) and flies at an altitude of approximately 693 km along a sun-synchronous near-polar circular orbit (Pham-Duc et al., 2017). The Sentinel-1 SAR mission has improved spatial coverage and revisits time compared to previous SAR system satellites, such as the ESA satellites (ERS-1, ERS-2, and ENVISAT-ASAR) and Canadian satellites (RADARSAT-1 and RADARSAT-2).

The main objective of Sentinel-1 satellites is to provide the continuous observation and monitoring of land and ocean surface all time (Veci, 2015). Sentinel-1 is designed to ensure consistent long-term data archive and conflict-free mode for flood mapping applications (Torres et al., 2012). The systematic acquisition strategy of the Sentinel-1 mission is more advantageous compared to the TerraSAR-X since it allows utilizing of continuous monitoring (Twele et al., 2016). The revisit cycle of Sentinel varies from 1 to 2 days over the western part of Europe. Table 1 below shows the historical characteristics of SAR systems of the past three decades compare to Sentinel-1.

Table 1: Satellite missions featuring SAR systems (Source: Grimaldi et al., 2016)

Mission/satellite	Agency	Years of operation	Ground resolution (m)	Revisit Interval (days)	Polarisation	Band
ERS-1	ESA	1991-2000	25	35	VV (single)	C
ERS-2	ESA	1995-2011	25	35	VV (single)	C
JERS 1	JAXA	1992-1998	18	44	HH (single)	L
RADARSAT-1	CSA	1995-2013	8-100	24	HH (single)	C
RADARSAT-2	CSA	2007	3-100	24	Full	C
ENVISAT-ASAR	ESA	2002-2012	30 - 1000	35	Single or dual	C
ALOS-PALSAR	JAXA	2006-2012	10 - 100	46	Single or dual	L
ALOS-PALSAR 2	JAXA	2014	3 - 100	14	Single or dual	L
COSMO-SkyMed	ASI	2007	15 - 100	16 (4 to < 1 with 4 satellites)	Single or dual	X
TerraSAR-X	DLR	2007	1 - 16	11	Full	X
TanDEM-X	DLR	2010	3	11	Full	X
KOMPSAT-5	KARI	2013	1 - 20	28	Full	X
SENTINEL-1A	ESA	2014	5 - 100	12 (1 - 6 with 2 satellites)	Dual	C
SENTINEL-1B	ESA	2016				

Sentinel-1 has four exclusive image acquisition modes: Interferometric Wide Swath Mode (IW), Wave Mode (WM), Strip Map Mode (SM) and Extra Wide Swath Mode (EW). Table 2 below lists the spatial characteristics of each acquisition modes. Among these modes, IW mode is widely used for monitoring of land surface and flood mapping purposes with dual polarization (Twele et al., 2016). IW is the primary acquisition mode for most of the overland applications (Potin, 2013). Sentinel-1 IW operates from an incidence angle range of 29.1° - 46.0°. Sentinel-1 also has different processing levels (Level-0, Level-1 & Level-2) and product types of Single Look Complex (SLC) and Ground Range Detected (GRD). Level-1 GRD products are projected to the ground range by means of an ellipsoid Earth model (Veci, 2015) and widely used in the area of flood mapping.

Table 2: Spatial characteristics of Sentinel-1 acquisition modes (Source: Sentinel-1 user handbook)

Acquisition Mode	Swath (km)	Spatial Resolution (m)
Interferometric Wide Swath	250	5 by 20 (single look)
Stripmap mode	80	5 by 5 (single look)
Extra Wide Swath mode	400	20 by 40
Wave mode	20 by 20 vignettes ground coverage	5 by 5
	100 along track distance between vignettes	

In addition to flood monitoring, Sentinel-1 satellites are also used for various purposes like forest and soil management mapping, routine sea-ice mapping, monitoring land-surface for motion risks, mapping to support humanitarian aid and crisis situations, surveillance of the marine environment and ship detection (Potin, 2013). Figure 2 shows an artistic view of Sentinel-1 when scanning the surface of the objects by emitting its own beam for various applications.

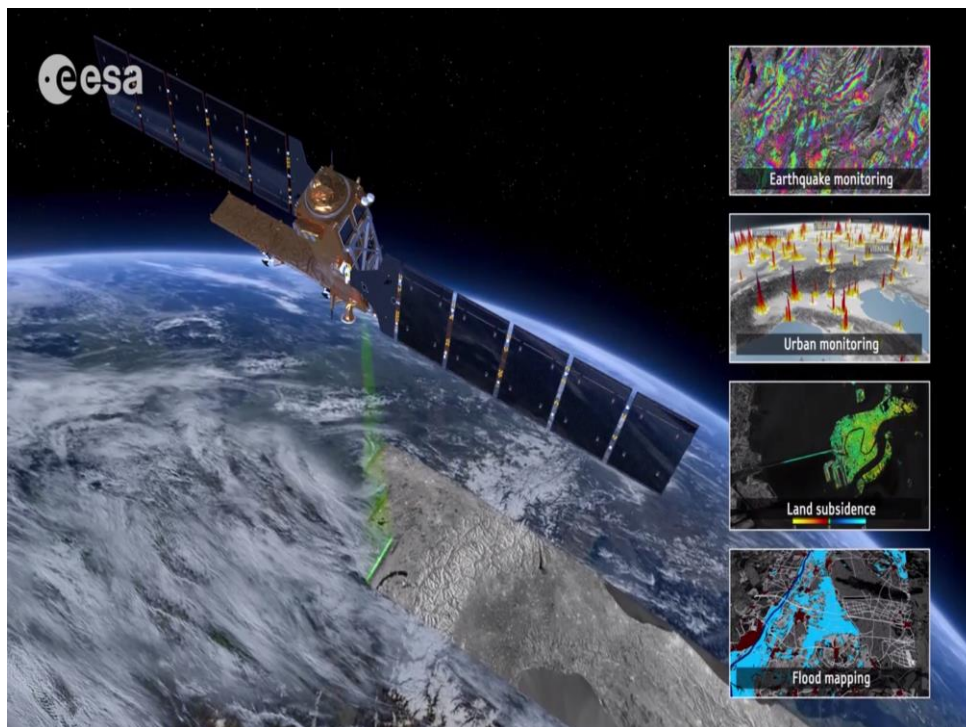


Figure 2: Artistic view of Sentinel-1 on the orbit scanning the earth surface (Source: <https://scihub.copernicus.eu/>)

### 2.3. Flood mapping from SAR imagery

SAR based flood mapping is considered as a suitable approach for flood monitoring (Twele et al., 2016). Because such sensors are independent of solar illumination and provide images during day and night (Manjusree et al., 2012). Since floods are often associated with extreme rainfall events with cloudy conditions, it will be impossible for optical sensors to acquire the needed information. However, SAR signals can penetrate clouds and rainy weather conditions, which makes them more attractive for near real-

time flood monitoring compares to the optical sensors (Smith, 1997). It is possible to detect floods in SAR images, because of specular reflection on the water surface (Gan et al., 2012). Water bodies appear as the black feature due to the low backscattering from relatively smooth water surfaces (Westerhoff et al., 2013). The interaction of water bodies and emitted signals are also influenced by acquisition parameters like wavelength, incidence angle, and polarisations. In recent years, high-resolution SAR systems, such as TerraSAR-X, RADARSAT-2, and COSMO-SkyMed SAR, provided very useful information for flood mapping purposes (Brown et al., 2016). The most recently launched Sentinel-1 SAR uses two satellites to provide improved temporal resolution products. However, mapping of water surfaces by Sentinel-1 is more challenging in comparisons to X-band SAR like COSMO-SkyMed, TerraSAR-X, TanDEM-X or KOMPSAT-5, this is because of the contrast of the water and non-water bodies decrease with the increase of wavelength (Twele et al., 2016).

Various semi-automatic and fully automatic SAR-based flood detection algorithms have been developed, which are even used for near-real-time flood monitoring. Some of these SAR based flood detections methods highlighted in literature include histogram thresholding (Brown et al., 2016; Henry et al., 2006), fuzzy classification (Martinis et al., 2015; Twele et al., 2016), texture analysis (Pradhan et al., 2014) and region growing (Martinis, Kersten, et al., 2015; Matgen et al., 2011) and change detection and thresholding (Long et al., 2014). The most of the methods mentioned here are using only a single SAR image for analysis of (Clement et al., 2017), so they are not able to present temporal variations flood extents. However, change detection approach can show the temporal variation of the flood extents (Byun et al., 2015; Giustarini et al., 2013; Hostache et al., 2012; Schlaffer et al., 2015).

For the improvement of flood extent extraction from SAR data, the thresholding approach can also be combined with various image processing techniques (Martinis et al., 2015). Recently, change detection and thresholding approach were introduced by Long et al. (2014), which was developed for Chobe floodplain in Namibia. This method is capable of showing the variations of flood extent over the time since it operated by using multiple SAR images. Clement et al. (2017) adapted this approach for multi-temporal Sentinel-1 images for a case study the United Kingdom and demonstrated the adaptability of the change detection and thresholding technique.

Thresholding technique is one of the most popular digital image processing, which classifies each pixel of the raster into water and non-water areas based on spectral characteristics as well as contextual and auxiliary information (Martinis et al., 2015). The effectiveness of the thresholding technique depends on the contrast between water and non-water areas, and it is examined through manual trial-and-error or automatically. Most of the previous studies used global thresholding technique since it is easy to carry out and faster because of less time required for computations (El-Zaart, 2015). Harmonic model (Schlaffer et al., 2015) and fully automated process chain (Twele et al., 2016) that used for near real-time flood monitoring were also applied with Sentinel-1 based flood mapping. Unfortunately, not all of these SAR-based techniques are equally applicable to all images because of their complexity, data requirements, their computational time and accuracies. In this study, thresholding technique is considered for the extraction of flood extents from multi-temporal images.

Polarizations has considerable effects on extraction of flood extents. Because polarization of sensors affects the amount of backscatter radiation returned to the sensors (Hostache et al., 2012). On previous studies Brisco et al. (2008) and Henry et al. (2006) used RADARSAT-2 and Envisat ASAR sensors respectively and shown that the HH polarization is more suitable for the flood extraction. Manjusree et al. (2012) also compared each mode of polarization for the RADARSAT-2 sensor on Bihar State in India and conclude that HH polarization is better for flood detection. On the other hand, Clement et al. (2017) and Twele et al. (2016) used Sentinel-1 SAR in Yorkshire, UK, and Evros River respectively and suggested that both VV and VH polarizations are useful for flood delineation.

## 2.4. Water level estimation from remote sensing

SAR-based flood maps are not only restricted to flood extents maps (Hostache et al., 2009). The availability of high spatial and temporal resolution of remote sensing imageries facilitate monitoring of spatially distributed surface water level dynamics from the space (Giustarini et al., 2011). Satellite remote sensing imageries have advantages over the in-situ measurement techniques regarding their spatial coverage (Clement et al., 2017). Mainly there are two approaches by which water levels can be derived from the remote sensing images, a direct and an indirect approach (Grimaldi et al., 2016). The direct retrieval of water level is obtained through SAR interferometry (InSAR), Radar altimeters and LiDAR directly while water level through an indirect approach is achieved by combining the flood extent map with a DEM (Hostache et al., 2009; Giustarini et al., 2011; Grimaldi et al., 2016).

Remote sensing based water level estimation provide advantages over intensive field measurement and for areas that are not easily accessible and poorly gauges. However, the remote sensing approach is a bit is difficult due to some issues like vegetation and buildings at the edge of the banks, resolution of DEM, image acquisition process (Barreto et al., 2016). The concept of integrating flood inundation map with high-resolution DEM has been achieved significant progress for the determination of water stage, which can be used for the flood modelling (Schumann et al., 2009). Usually, water level data derived from the remote sensing images are used for comparisons with in-situ water level measurements and also for calibrations, validations and data assimilation for the hydraulic models (Grimaldi et al., 2016). The accuracy of water levels retrieved from remote sensing by the indirect method is influenced by the factors like quality of flood maps and DEM resolution.

The studies performed by Matgen et al. (2007) for Alzette, Luxembourg showed root mean square error (RMSE) of 41 cm in water levels using ENVISAT ASAR. Another study over six Canadian lakes by Nielsen et al. (2017) shows nice agreement with in-situ water level with the RMSE value range from 5 to 68 cm for CryoSat-2 and 17 to 54 cm for ENVISAT. They have used SAR Interferometer Radar Altimeter (SIRAL) for CryoSat-2 and Radar Altimeter 2 (RA-2) for ENVISAT for their study.

### 3. STUDY AREAS AND DATA SETS

#### 3.1. Study Areas

The study is conducted in two areas located in Overijssel province, in the Netherlands. These areas are managed by two different Dutch regional water management authorities namely Waterschap Drents Overijsselse Delta and Vechtstromen (see Figure 3 for their location). The topography of the study areas is almost flat. For retention reservoirs study area, some of the places lay below mean sea level with the range of - 3 m a.s.l and 15 m a.s.l.. In case of the Dinkel river, the elevation varies from 26 m to 44 m a.s.l.. The study areas have almost the same weather conditions. The mean monthly temperature vary from approximately 3 °C to 17 °C in January and July, respectively. They are also characterized by evenly distributed precipitation throughout the year with the mean annual sum of 765 mm. Land use land cover of the areas consists of agricultural land, forest, and urban areas.

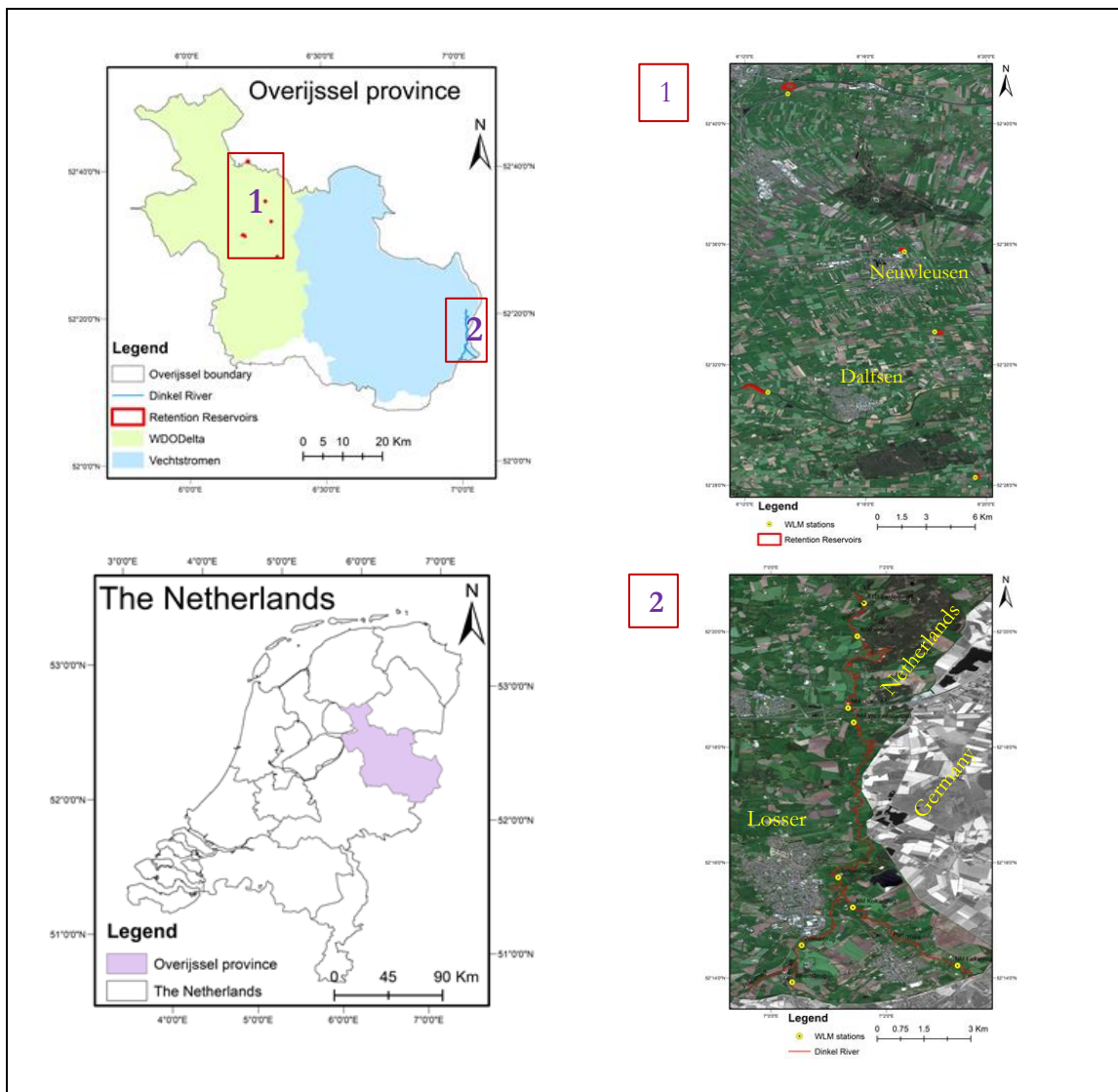


Figure 3: Study area maps: retention reservoirs (upper right, 1) and Dinkel river (lower right, 2) with the background image of Sentinel-2A acquired on May 08, 2016 (available from online map)

Each regional water authorities have the same intended purpose (for mitigation of the flood) but from different perspectives. In the case of WDODelta, they mainly focus on flood mitigation through the aid of flood retention reservoirs. When there are extreme flood events, flood water will be diverted into the retention reservoirs. Then, the retention reservoirs serve as the room for water to delay the floods and gradually released to minimize the consequences of water excess situations. The Vechtstromen regional water authority is interested in monitoring the floods of Dinkel catchment from both farmers and waterboard perspectives to preserve the nature and minimize the effects of the floods. The occurrence of the flood is not limited to the winter season; it also happens sometimes during the summer period.

The Dinkel river is a transboundary river that flows from Germany into the Netherlands and then back into Germany as a tributary of Vecht, river which finally back to the Netherlands again. This river suffers from riverine flooding occurs as a consequence of runoff exceeding the capacity of its channels. The upper part of the river experiences floods mainly in the months from November to March. Dinkel area is one of the 24 areas designated as Natura 2000 area in the Overijssel province. Natura 2000 is the project of European Union that focus on protections of flora and fauna and financially contributed by the European Commission. Therefore, Dinkel catchment management can comply with the Natura 2000 regulations.

The WDODelta water management authority has a number of retention reservoirs for flood mitigation. Each reservoir varies in size and shape. For this study, five retention reservoirs were selected based on their size and availability of water level stations. The shape of reservoirs affects the detectability of the reservoirs from Sentinel-1 SAR resolution. It is difficult to observe the retention reservoirs having a narrowly elongated feature like a canal. Therefore, such conditions were also considered when the selection retention reservoirs. Table 3 shows the information such as surface area, elevation range, and locations of each selected retention reservoirs for this study.

Table 3: Retention reservoirs characteristics

S.No.	Reservoir ID	Surface area (ha)	Elevation range (m)	Location coordinates (degree)	
				Latitude	Longitude
1	DV0277/79	2.601	1.48 - 4.07	52.595° - 52.599°	6.284° - 6.290°
2	HV0001	11.687	-0.39 - 2.21	52.685° - 52.690°	6.220° - 6.228°
3	OK0302	1.079	3.15 - 4.79	52.470° - 52.473°	6.327° - 6.330°
4	OV0002	4.257	-0.02 - 4.79	52.515° - 52.526°	6.197° - 6.214°
5	SZ0265	1.855	1.98 - 3.46	52.549° - 52.553°	6.306° - 6.310°

### 3.2. Data Sets

#### 3.2.1. Multi-temporal Sentinel 1 SAR Images

One of the main input data for this research is Sentinel-1 SAR images. These products are downloaded from European Space Agency (ESA) Copernicus Open Access Hub page. The Sentinel products are open and free to the public. The free access to the page: (<https://scihub.copernicus.eu/dhus/#/home>) granted after one-time registration.

Sentinel-1 SAR images since from the operational time of Sentinel-1A and 1B, which means from October 03, 2014 to June 08, 2017 were downloaded. After initial processing of all the downloaded images, finally, 50 images for Dinkel river and 79 images for retention reservoirs were selected based on flood condition for further analysis. The product in the mode of Interferometric Wide swath and Level-1 Ground Range Detection were utilized in this study. The IW mode was chosen since it is the main acquisition mode over the land surface. Additionally, Sentinel-1 user handbook by Potin (2013) indicates that IW mode can use for flood monitoring application. Regarding the product levels and types, Level-1 GRD was selected, because it is multi-looked and projected to the ground range using an Earth ellipsoid model. Level-1 IW GRD high resolution has a 5 x 1 number of looks, 250 km Swath, 5 x 20 m<sup>2</sup> spatial resolution and 10 x 10 m<sup>2</sup> pixel spacing in (range x azimuth). Over the study areas, Sentinel-1A and 1B operate in the dual polarization mode (VV/VH). Table 4 summarizes some details in interferometric wide swath mode.

Table 4: The main characteristics of Sentinel-1 Interferometric Wide swath mode (Source: Sentinel-1 user-guide)

Parameter	Interferometric Wide swath mode (IW)
Swath Width	250 km
Incidence angle range	29.1° - 46.0°
Sub-swaths	3
Azimuth steering angle	± 0.6°
Polarization options	Dual VV+VH
Maximum Noise Equivalent Sigma Zero (NESZ)	-22 dB
Radiometric stability	0.5 dB (3 $\sigma$ )
Radiometric accuracy	1 dB (3 $\sigma$ )
Phase error	5°
Pixel spacing	10x10 m

#### 3.2.2. Digital Elevation Model

In this study, DEM was used to estimate the water level with the combination of flood extent maps. In order to compare and verify the reliability of the flood extent maps generated from Sentinel-1 SAR with the in-situ water level measurements, a high-resolution DEM is required. Hence, a high-resolution DEM with a comparable resolution as the Sentinel-1 image is needed. Fortunately, the Netherlands have very high-resolution DEM generated using laser altimetry.

The current Altitude File Netherlands, version-2 (AHN2) DEM which is translated from the Dutch language “Actueel Hoogtebestand Nederland” has the spatial resolution of 0.5 m, which is even higher than Sentinel-1 IW resolution. A ground level filled and non-ground object removed 0.5 m AHN2 DEM product type data were downloaded from the Public Services On the Map (PDOK) website: (<https://www.pdok.nl/>) and processed to match the resolution of Sentinel-1. After downloaded AHN2 DEM, twenty-eight files for WDODelta and six files for Vechtstromen, the individual file were mosaicked

into one file and cropped to a specific area of interest, (see Figure 5). Then, in order to match the DEM resolution with the one of Sentinel-1, they are resampled into 10-meter resolution using ArcGIS. The whitish spots indicate that the place where there is no DEM data because the product utilized is the raster data wherein all non-ground level objects like buildings, bridges, trees, and others have been removed from the point cloud. Filling these gaps may result in an inaccurate result. Therefore, it was decided to use as it is and resampled into the intended resolution. Figure 4 and Figure 5 show the DEM of Vechtstromen and WDODelta, respectively. The topography of retention reservoirs study area is quite flat, and even someplace fall below sea level. Based on the available continuous measurement of the water levels, only five stations were used for Dinkel river study area.

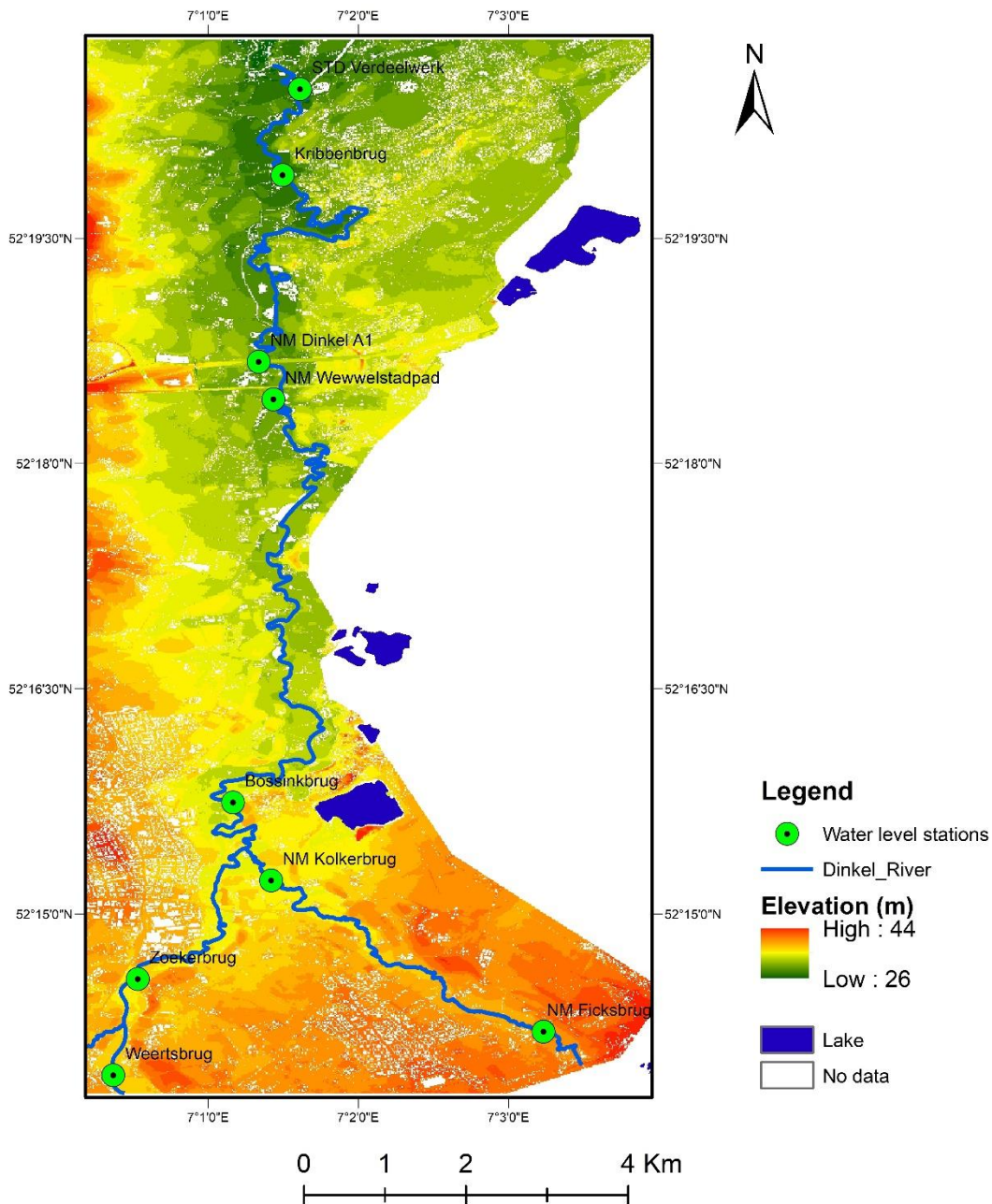


Figure 4: DEM for Dinkel study area mosaicked from six AHN2 DEM tiles.

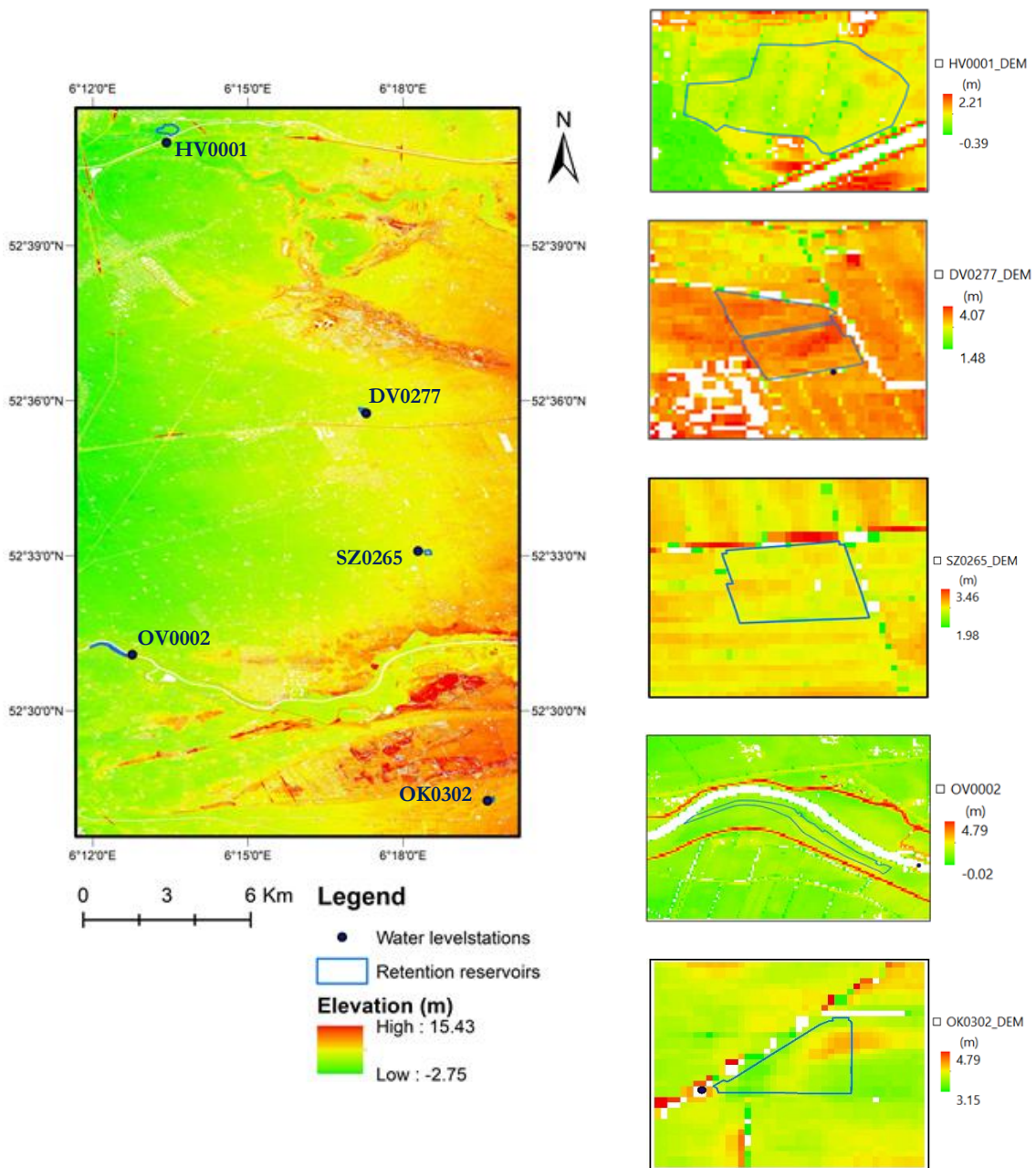


Figure 5: DEM for retention reservoirs mosaicked from twenty-eight AHN2 DEM tiles and shows the locations of each retention reservoirs with their elevation

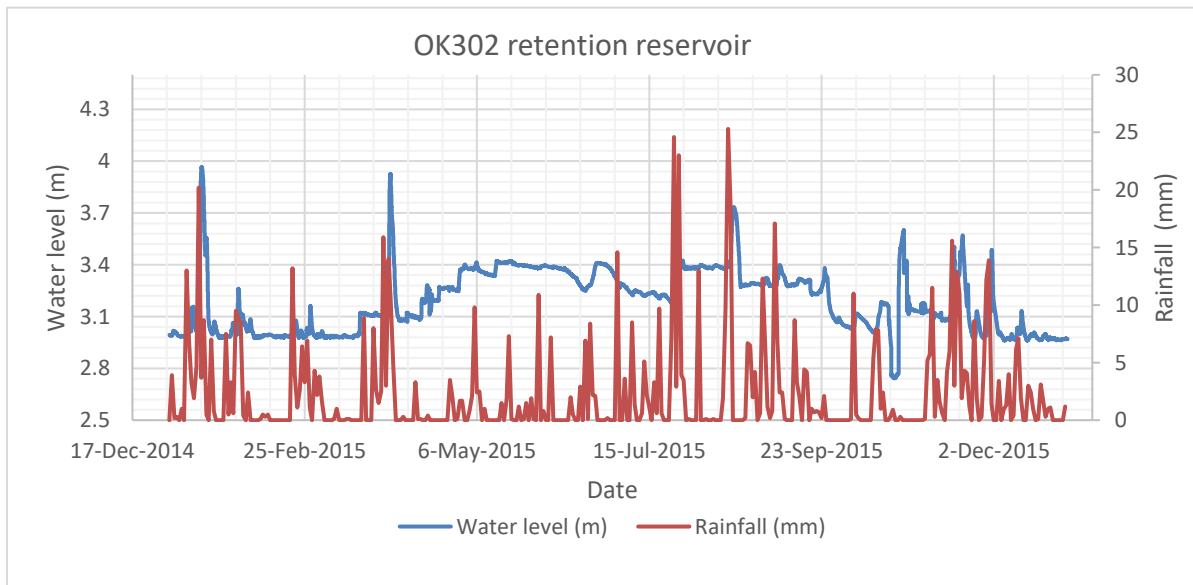
### 3.2.3. Water Levels Measurements

The in-situ water level measurements for flood retention reservoirs were provided by Drents Overijsselse Delta water authority (see Figure 5 for the locations). The in-situ water level measurements of the Dinkel were provided by Vechtstromen regional water authority (see Figure 4 for the locations). According to the available information from the water authority not all available reservoirs supposed to be studied have regular water level measurements. This issue affects the selection of reservoirs for this study in addition to the issue of the size of the reservoirs Since Sentinel-1 is not able to detect clearly if the size of the reservoirs is less than 10 meters and narrowly elongated reservoirs like as canals. Hence, five larger reservoirs having an area more than one hectare and water level measurement were selected.

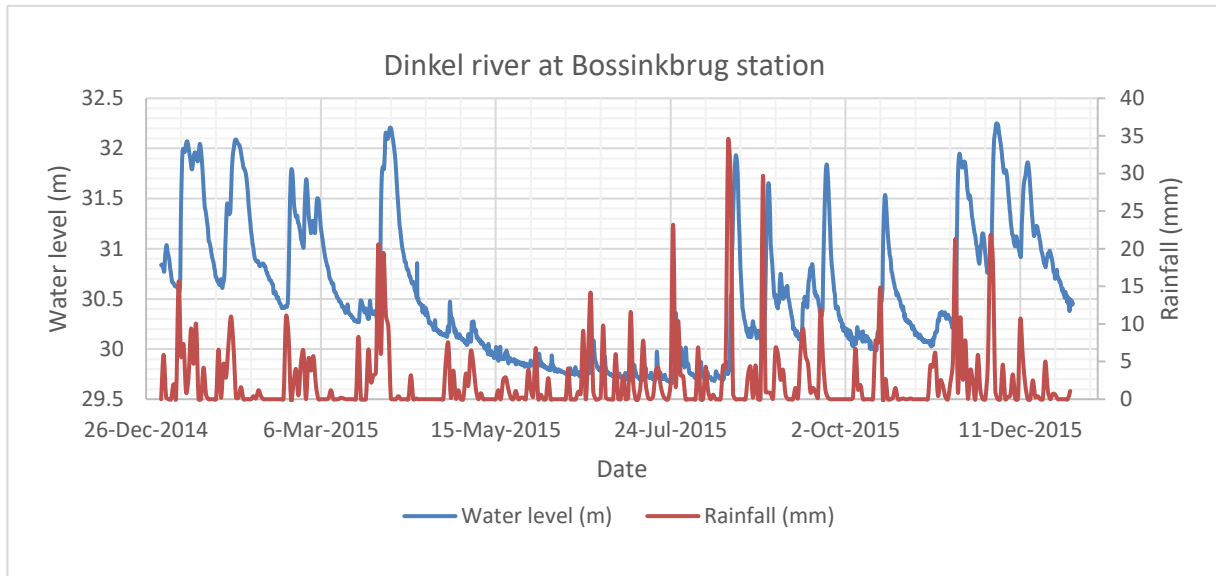
In the case of Dinkel river, there are no limitations like with the retention reservoirs in WDODelta. But, some stations have no continuous water levels measurements. Due to this case, only five stations which having enough recorded data were selected. The water level data were obtained from October 2014 to August 2017 for each area. The measurements have an hourly temporal resolution which gives detailed information on the variation of water levels. This in-situ water level measurement will be finally used to verify the accuracy of the water levels estimated from a combination of flood maps and DEM. The sample water level measurement with rainfall data for 2015 is shown in Figure 6.

### 3.2.4. Rainfall measurements

The weather data (rainfall data) were accessed from Royal Netherlands Meteorological Institute (KNMI) website: <http://www.knmi.nl/nederland-nu/klimatologie-metingen-en-waarnemingen>. For this study rainfall data from October 2014 to September 2017 were collected at Heino station for the retention reservoirs in WDODelta and Twente station for the Dinkel river. Having this data provides information about dry and wet seasons and occurrence of heavy rainfall events, which helps to understand the occurrences of the floods. Figure 6 shows sample data taken from each study area. From these graphs, we recognize that the peak of water level corresponds to the peak rainfall.



(a) Ok0302 retention reservoir water levels and rainfall measurements (Heino weather station) during 2015



(b) Bossinkbrug station water levels and rainfall measurements (Twente weather station) during 2015

Figure 6: Water levels and rainfall data were taken for the 2015 year over (a) retention reservoir OK0302 and (b) Dinkel river at Bossinkbrug

Depend on the weather forecast, the water retained in the reservoirs may stay for some time from water management point of view in the case of WDO Delta. Hence, some reservoirs may hold water during the summer period. When there is heavy rainfall expected, they released the water within the reservoir gradually. From Figure 6, (a) we can observe that the water level on February month is kept lower and increased at the start of summer period after a high rainfall event.

## 4. SENTINEL-1 SAR PRE-PROCESSING AND METHODS

Remote sensing based flood mapping using SAR imageries are well recognized for their capability to detect the floods. However, retrieval of useful information from the images is not an easy task. An intensive pre-processing is needed to correct for the effect of speckle due to interference and geometric distortion due to the terrain. In order to achieve the overall objectives of the study, the methodology, which includes Sentinel-1 pre-processing as shown in Figure 7 was followed.

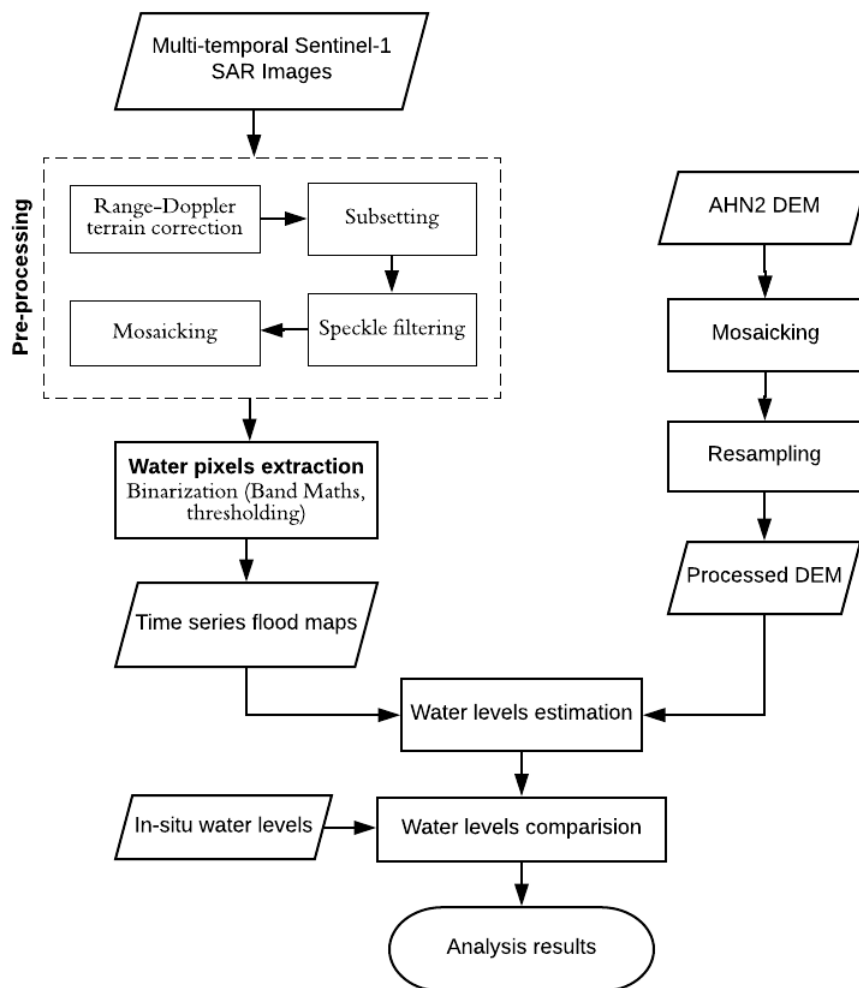


Figure 7: Flowchart of the research methodology used for performing flood mapping and water level estimation from multi-temporal Sentinel-1 SAR images

Time series of Sentinel-1 SAR images downloaded from the website were passed through pre-processing steps as shown in Figure 7. Then, in order to produce time series flood extent maps, global thresholding technique which identifying water and non-water areas were used. To verify the reliability of the Sentinel-1 SAR detects flood extents, the flood maps generated from SAR were combined with digital elevation model to determine of water levels. Finally, the water levels obtained from the flood maps were compared with in-situ measured water levels. Details of each part of the methods are described in the subsequent sections.

#### **4.1. Sentinel-1 SAR pre-processing**

The flood maps derived from SAR observations need a number of pre-processing steps before it can be used for further assessment. The pre-processing applied for this research is described in the subsequent sections. The freely available, Sentinel Application Platform (SNAP) toolbox, provided by ESA was used to perform image processing and analysis of the data. ENVI IDL software was also used to perform image subsetting and mosaicking in addition to SNAP toolbox.

##### **4.1.1. Range-Doppler Terrain Correction**

Radar systems are operated by the side looking at the objects. Due to this case, Sentinel-1 SAR images suffer from geometric distortion such as foreshortening, layover and shadow effects. The geometric distortions are most dominant on the mountainous topography in compared to the flattened areas. In our case, the study areas are an almost flattened area, therefore, there is not thus much serious geometric distortion. However, geometric correction is needed in order to put the correct position of each pixel. The geometric distortions of the images should be removed before using SAR images further applications such as flood mapping, using terrain correction (Logan & Facility, 1995). Therefore, terrain corrections are intended to be applied to the images before some other pre-processing steps like mosaicking. Terrain correction for this research was applied using SNAP toolbox Range doppler terrain correction tool (Veci, 2015). There is some advantage of using range doppler terrain correction from SNAP toolbox (Bayanudin & Jatmiko, 2016), as described below.

The range doppler terrain correction tool in SNAP performs multiple tasks. These consist of corrections for topographical variations and tilt of the satellite sensor (orthorectification) and radiometric normalization. Furthermore, the tool also calibrates the pixel value to radar backscatter and projects the image to the correct position relative to the north. In the SNAP toolbox, the range-doppler terrain correction uses the SRTM 3 sec DEM and bilinear interpolation resampling. The terrain geocoding involves using this DEM to correct the inherent SAR geometric distortions (Veci, 2015). (see Appendix B)

##### **4.1.2. Speckle Filtering**

Speckle noise is the grainy salt-and-pepper effect present in radar images that occurs due to the random interference of electromagnetic waves (Qiu et al., 2004). It is happening because of coherent processing of returned backscattered signals from a multiple distributed target due to which constructive and destructive interference appear as bright and dark dots in the images. Speckle effect is one of the serious problems in SAR images, which degrades the quality of the images and makes analysis, interpretations, and classifications of the image difficult. Therefore, reduction of speckle noise is essential before utilizing the SAR images for further applications.

There are several speckle reduction techniques developed for SAR images. However, not all the available techniques perform the same regarding speckle suppression, and edge and feature preservation at the same time. Hence, there is no single filtering technique to be selected as the best speckle filter. Previous studies by Lee et al. (2009) and Meenakshi et al. (2011) shows that Lee Sigma filter performed better than the other speckle filters. In another study, Long et al. (2014) indicated that Gamma (maximum a posteriori – MAP) is a nice speckle filter since it requires relatively low processing time, and is effective for SAR sensor modes, angles, and resolutions.

The objective of speckle suppression is to remove speckle noise. However, the best speckle suppression techniques may reduce the spatial resolution of the images which may lead to loss of spatial detail. The speckle suppression by Lee, Frost, and Gamma-MAP perform nicely, but there are difficulties when it is required to preserve the image details at the same time with these speckle filtering (Yommy et al., 2015). Therefore, it is essential to give attention to speckle filtering to preserve detail information. Compare to

the other speckle filter types; the Refined Lee is capable of preserving the linear features, edges, texture information and point targets in addition to despeckling (Yommy et al., 2015).

Performance of speckle filters can be assessed both quantitatively and qualitatively. The quantitative assessment evaluates how efficient speckle filters suppress the speckle, preserve the edge, and preserve the fine details of features (Sheng & Xia, 1996). Visual inspection is used as a qualitative assessment that is a quick and efficient way to assess the performance of speckle filtering techniques. In general, the main idea is to adopt the speckle filter that suppresses the best speckle and at the same time that preserves the edges.

The SNAP toolbox provides eight speckle filtering techniques. Each filtering was tested for the same area of interest to select the speckle filter perform better based on visual inspection in addition to the literature review. Figure 8 shows the effect of the speckle filters tested near to one of the retention reservoirs (OV0002) along Vecht river, with nearby features like a bridge and a road. Lee-Sigma (Figure 8) highly smoothens the image and results in a loss of spatial resolution, it is considered as the worst filter here. However, Refined lee is smoothed out the spikes while maintaining the spatial structure of the signal. Hence, it was selected as the best filter and used for this study.

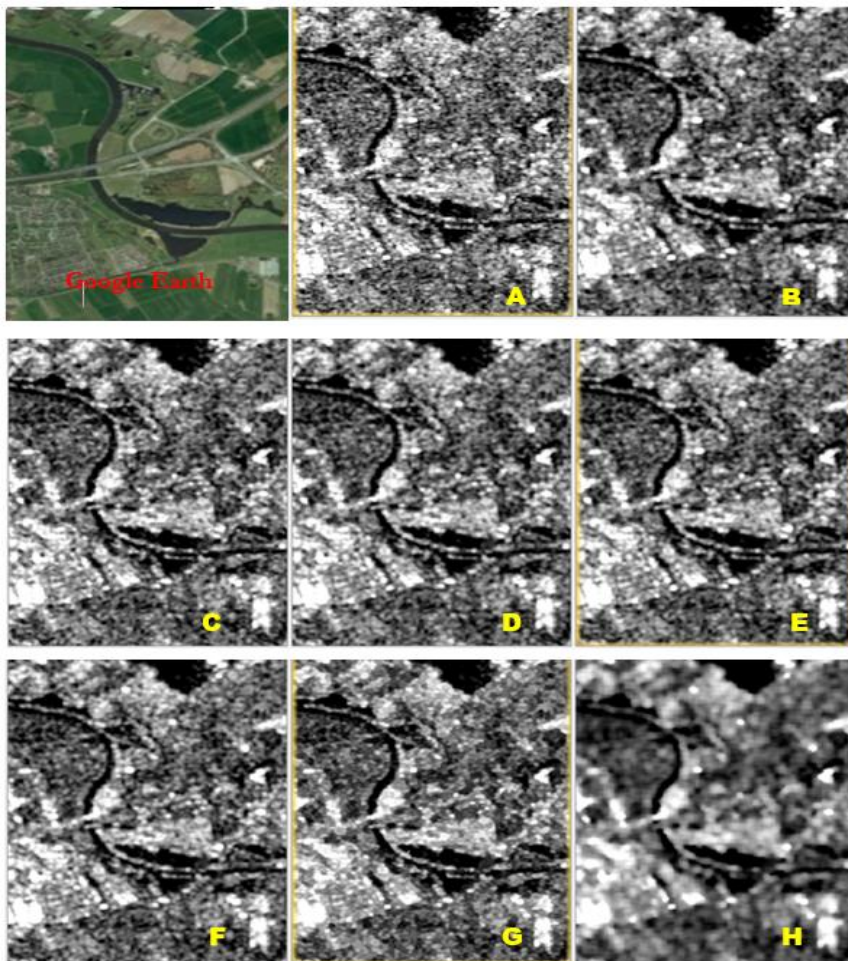


Figure 8: Speckle filtering test for image taken on December 22, 2014, near to OV0002 retention reservoir, (A) Terrain image (B) Boxcar (C) Median (D) Frost (E) Gamma-MAP (F) Lee (G) Refined Lee and (H) Lee-Sigma

#### 4.1.3. Subsetting and Mosaicking

Subsetting is an operation which is used to speed up the computational time for the remaining steps since it reduces the extent of the image that needs to be analysed. The original product of Sentinel-1 SAR product downloaded from the Copernicus Open Access Hub page is obviously larger than the area of interest. Therefore, to remain with the areas of interest, it should be subsetting to the specific extent. For this research, the Sentinel-1 images were subsetting to the study area of Dinkel river by a rectangle between the coordinates of longitude  $6^{\circ}58'00'' - 7^{\circ}05'21''$  E and latitude of  $52^{\circ}13'10'' - 52^{\circ}23'44''$  N. The study area for retention reservoirs are cropped on longitude  $6^{\circ}07'00'' - 6^{\circ}23'00''$  E and latitude of  $52^{\circ}15'00'' - 52^{\circ}42'00''$  N. Each retention reservoir is cropped into their areal extent to present the results individually.

During downloading the satellite images, single downloaded images may not cover the whole area of interest in some cases. Therefore, the multiple images may be mosaicked into to one in order to fit the area of interest. The mosaicking step is needed to be applied only to those images do not cover the entire area of interest. Most of the downloaded images were cover the area of interest. Hence, only a few images were undergone the mosaicking step.

#### 4.2. SNAP graph builder

Applying all these above mentioned pre-processing steps for each image one by one will obviously consume a considerable amount of time. Hence, SNAP graph builder operation was used to develop batch processing (see Appendix B). The developed batch processing graph is capable of performing multiple tasks in sequence. Figure 9 shows the batch processing graph developed for range doppler train correction, subset, and speckle filtering. Unfortunately, there is no option to create batch processing for mosaicking operation in SNAP. Therefore, it was done separately for only those images needs mosaicking.

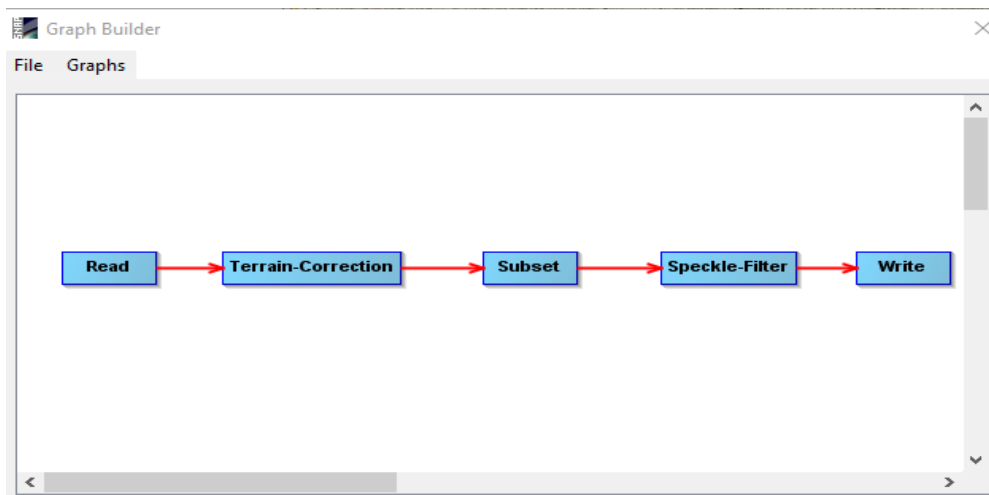


Figure 9: Sentinel-1 SAR Batch processing orders on SNAP graph builder.

## 5. OPEN WATER DETECTION

### 5.1. Water surface backscattering mechanisms

Detection of the water surface is a function of many parameters, mainly surface roughness, dielectric properties, polarization, wavelength, and incidence angle. Surface roughness is one of the factors which determines the amount of radar backscatter. Smooth surfaces mainly result in low backscatter because of specular reflection away from side-looking SAR sensor (Schlaffer et al., 2015). Therefore, the images of smooth surfaces appear as dark pixels. In contrast, no rough surfaces have high backscatter signals, which appear as bright pixels in radar data (Gan et al., 2012). This means as the surface roughness increases; backscatter will also increase. The roughness of the object is not only characterized by its geometric properties but also depends on the local incidence angle and wavelength of the signal (Martinis, 2010). Furthermore, the backscatter signal also depends on dielectric properties of the surface of the object. Water has high dielectric constant which causes high resistance to be penetrated by the radar signal and result in the low backscatter value. The backscattering mechanisms under different water and land conditions are illustrated in Figure 10.

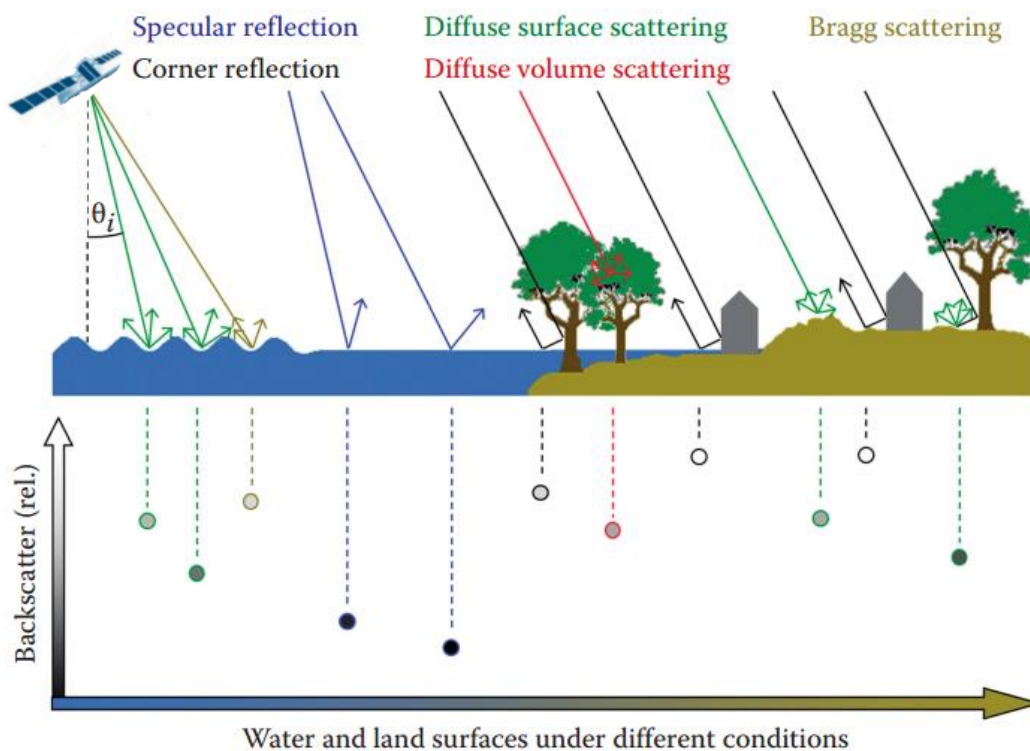


Figure 10: Backscattering mechanisms over water and different surface condition. Specular reflection over the water body is shown as very low backscatter (Source: Martinis S., 2010)

Generally, open water bodies are considered as perfectly smooth surfaces. However, in the case of submerged vegetation, wind and rainy conditions the surfaces of the water do not remain as the perfect smooth body and increase the backscatter signals. This condition may lead to misclassification of the flooded area as non-flooded area. However, VV polarization will decrease such misclassification since it is sensitive to small vertical variation in compare to HH polarization mode.

## 5.2. Sentinel-1 SAR polarization

SAR polarization refers to the way in which the radar waves are being transmitted and received along the geometric plane. Polarization is one of the main important SAR parameters that influence detection of the floods. Generally, HH polarization is considered superior for discriminating water bodies from other land surface compared to other polarization. This is because of low backscattering signal from the open water surface in horizontal component (Martinis, 2010). However, HH is not any more effective when there is the issue of surface roughness occurs due to conditions like wind and submerged vegetation.

The HH polarization is systematically not available for Sentinel-1 IW products. Over the study areas, Sentinel-1 IW mode has acquired the images in the form of VV/VH polarized. In order to choose the polarization mode which is more appropriate for flood detection, the comparison needs to be done between VV and VH polarization. Recently, research based on Sentinel-1 flood mapping performed by Twele et al. (2016) on Greece/Turkey compared the mapping capability of VV/VH polarization. They conclude that VV polarization is slightly better than VH polarization. Another study by Psomiadis (2016) also showed that better results were obtained from VV polarization in comparison to VH for Sentinel-1.

Furthermore, the research done by Manjusree et al. (2012) also shown that VV polarization has high potential to identify partially submerged vegetation since it is more sensitive to surface roughness. However, they have used ENVISAT products. This indicates that sensors polarization is behaving almost the same regardless of the sensors type. For this study, the visual inspection of VV polarization has been seen more realistic than VH when it is observed from multi-temporal SAR images, see Figure 11. There is no doubt to adopt VV polarization for flood extraction as it is observed from the comparison on Figure 11. In general, based on the visual assessment from the time-series and the acknowledgment of those references, VV polarisation mode was selected for this study.

## 5.3. SAR-based flood extent extraction technique

Numerous techniques have been developed to extract water bodies from SAR imagery. However, based on their degree of complexity, data requirement and computational time needed, they are not equally appropriate. Thresholding method is one of the most widely used digital image processing technique. It classifies each pixel of the image into water and non-water areas based on their spectral characteristics. For improvement of flood extent extraction, thresholding approach can also be combined with other techniques like change detection (Martinis et al., 2015). The combinations of change detection and thresholding technique is advantageous for the multi-temporal flood mapping, since the change detection utilized multiple images as flood and reference images in order to show temporal variation of the floods. However, selection of an accurate reference image (non-flooded image) image is a difficult task. Once the wrong reference image was selected, the error/misclassification will be propagated through all the time series flood maps and result in wrong information.

The change detection and thresholding technique, which developed by Long et al. (2014) for Chobe floodplain in Namibia were proposed to be used for this study previously. However, this technique requires some further processing steps in addition to the challenge behind the selection of reference image. According to this approach, the image acquisition mode has to be the same orbital pass (track) to analyze in order to avoid high variation of incidence angles. To remove water look-alikes, unlikely flooded areas are expected to have a higher slope. The height above nearest drainage (HAND) is developed from DEM to help to distinguish flooded areas and water look-alikes. The criteria that determine whether the pixels are flooded or non-flooded comprises an empirical coefficient which needs to be optimized for the specific study area. However, performing all these steps mentioned above for all available Sentinel-1 SAR images costs a considerable amount of time. In compared to the other techniques, histogram thresholding is very fast and high potential for automation with moderate complexity. One of its limitation is, it may fail

in the case of very low contrast between water and non-water surfaces. In general, histogram thresholding technique is considered as adequate for flood mapping generation for this research.

From the multi-temporal analysis, it is recognized that not one single threshold value is valid for all images of different dates and location. This is because of environmental conditions like windy and rainy conditions and also because of different incidence angles. Over the study area, Sentinel-1 has acquired the images in four real orbit track which called, track-15 and track-88 in ascending pass and track-37 and track-139 in the descending pass. These passes have different incidence angle which influences the magnitude of backscatter signals and as a consequence the selection of threshold values. The effectiveness of the extraction of flooded pixels by thresholding technique depends on the contrast between the backscatter of the water body and land surface.

SNAP toolbox band math operation has been used to binarize (segment) the images into a flood and non-flood pixels by means of manual trial-and-error. Backscatter analysis was done from VV-intensity in decibels (dB). Using histogram view and band math calculation, discrimination of water and non-water pixels has been performed. In order to binarize the images, a logical statement was used to return value 1 for water and 0 for non-water for a specified value of the threshold. The threshold value that was used for flood mapping for this study ranges from -18 dB to -14 dB. Three class of threshold values were applied for all images first, then by critically looking at the Sentinel-1 images visually, adjustment of threshold has done for those need adjustment in order to extract the appropriate flood extent. Compared to other land surfaces (rough), smooth water bodies have very low backscatter values (see Figure 10).

Figure 11 show comparisons of VV and VH polarization for the image taken on February 24, 2016. The rest of the time series images indicate the same behaviour. As it is visualized from the image (red circle), it is indicating permanent water body (lakes). From this observation, the capability of VH in identifying water from non-water is very low compared to VV. The histogram for VH does not really indicate the separation of water and non-water since the contrast between water and non-water is very poor. We can also understand the weakness of VH from the shape of the histogram. However, in the case of VV, the histogram shows demarcation of water from non-water bodies (see red arrow). In generally, discrimination of flooded and non-flooded pixels was achieved using VV polarization mode. Band maths operation (binarization) technique were applied in order to create final flood maps. The same steps were followed for other images to generate the time series flood maps.

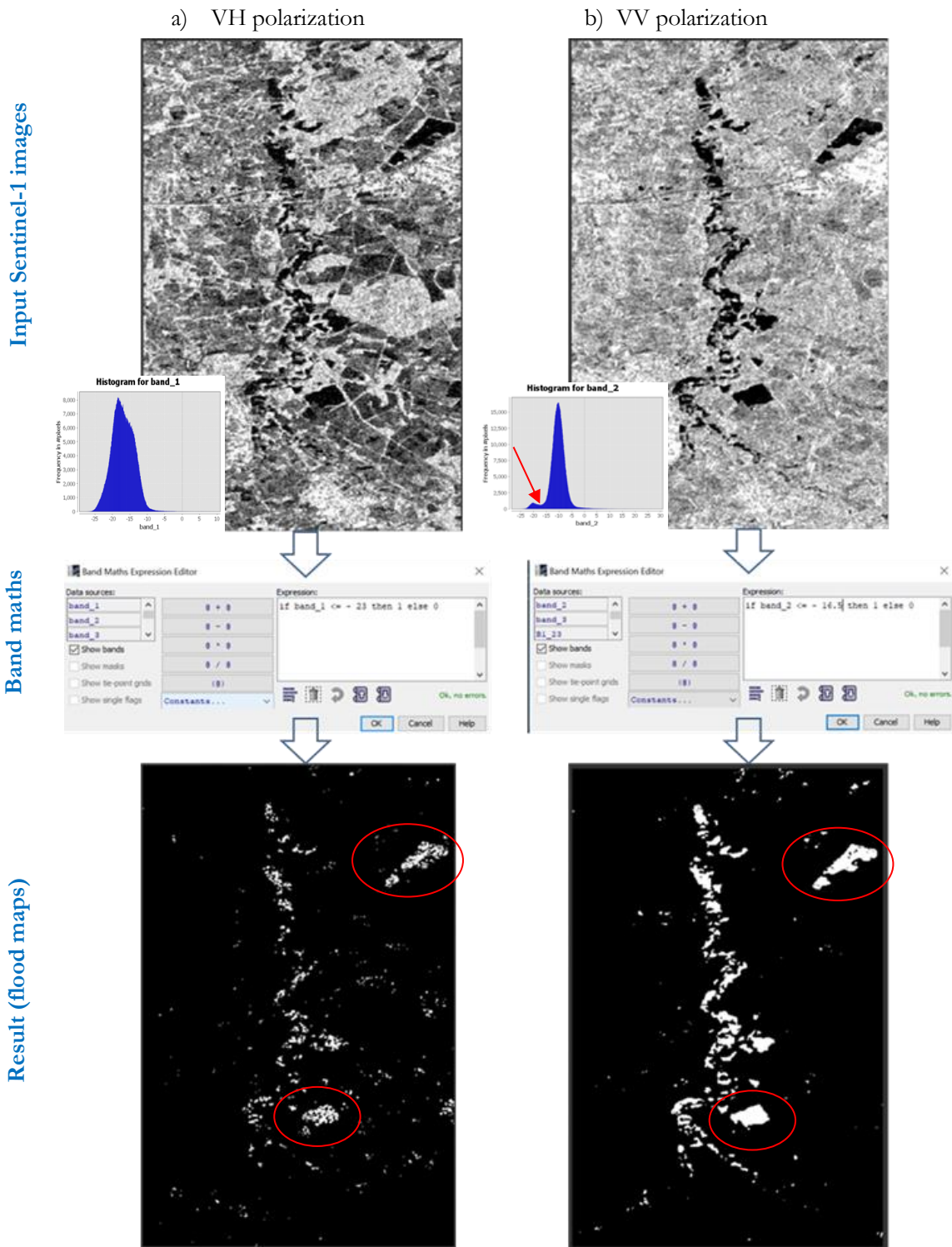


Figure 11: Comparison of VH polarization (a) and VV polarization (b) for the images taken on February 24, 2016, over Dinkel catchment (red circle indicates permanent water, lakes)

## **5.4. Sentinel-1 SAR flood maps**

This section presents and explains the flood map time series results were generated for Dinkel river and retention reservoirs. The time-series images used for this study are listed in Appendix A.

### **5.4.1. Dinkel river time series flood maps**

According to the time series flood extent assessment done from October 2014 to March 2017 in this study, the peak floods happened on February 24, 2016, and covered an area of 131 hectares along the banks of the Dinkel river. The surface area of the flood was calculated within the extent of 400 m buffering to Dinkel river shapefile digitized from google earth map. The second highest peak flood occurred on December 2, 2015, and flooded 121 hectares of land.

Because of its narrow width, which is less than the resolution of Sentinel-1, it was not possible to observe Dinkel river itself unless there is a flood. From a visual inspection of downloaded multi-temporal images, most of them were identified as dry images. In order to generate flood maps, setting the proper threshold value is significant. In fact that not only single threshold value is not valid for all images. Setting up the threshold value manually by trial and error for all pre-processed requires a considerable amount of time. Therefore, based on an initial analysis of the 338 pre-processed images only 50 images, which corresponds to flood events were used. Mainly the images within winter period, November to March months were selected for the flood mapping. All the flood maps generate were used to for the development of flood frequency map. They have also used for generation linear regression with in-situ water levels to verify the reliability of generated flood maps. In order to show the spatial and temporal variability of flood extent in this study, some of the images are presented in Figure 12. Sentinel-2A mosaicked image for the Netherlands acquired on May 08, 2016, which is available from the online map was used as the backroad image for all flood maps generated for each study areas.

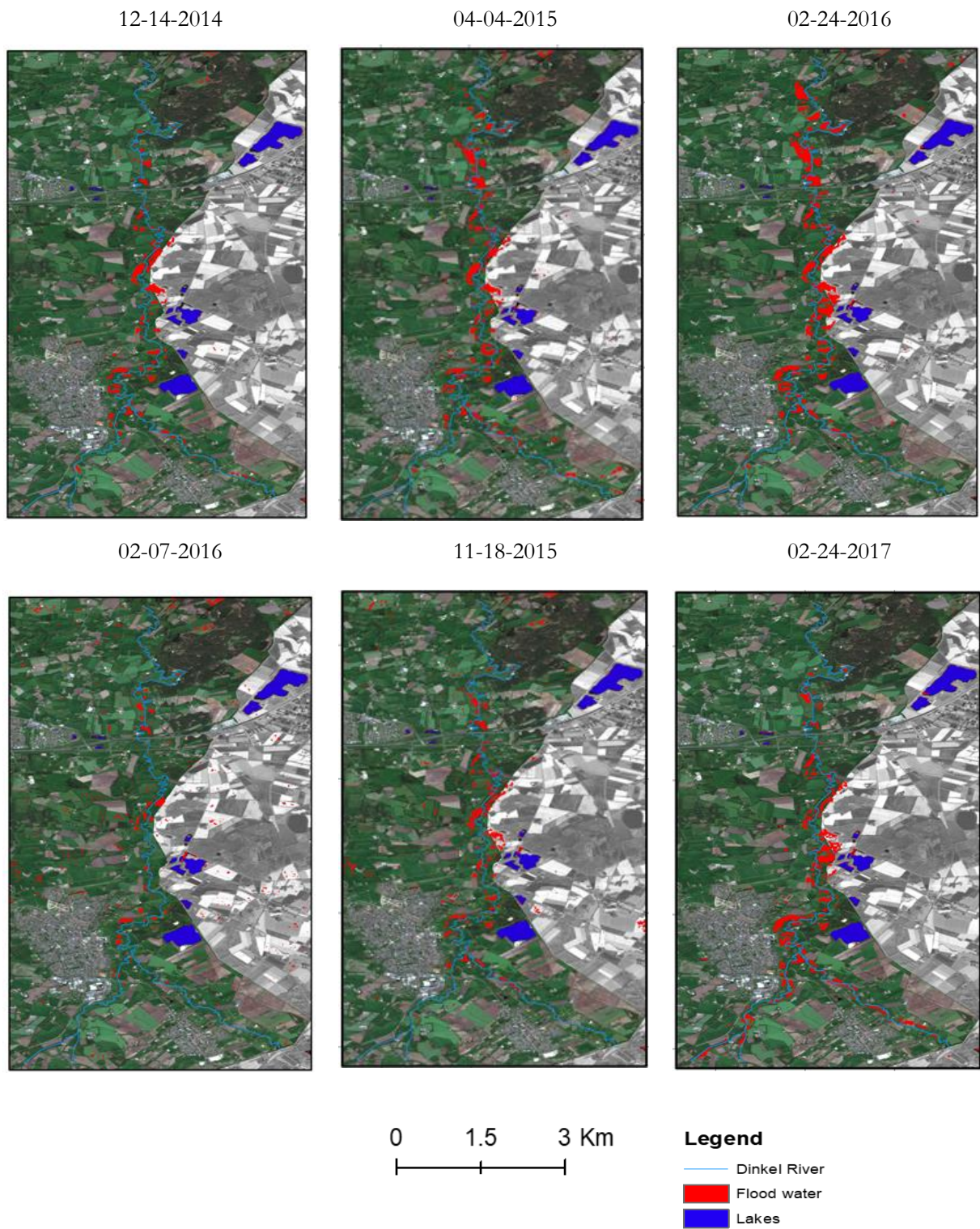


Figure 12: The flood maps for Dinkel river shows approximately some low, medium and high flood with the background image of Sentinel-2A acquired on May 08, 2016 (available from online map)

Figure 13 shows the photograph of the flood captured by drone for the flood occurred on February 24, 2017, near to the Losser city. The flood at this date was covered an area of 103 hectares.



Figure 13: Photograph of the Dinkel flood captured on February 24, 2017, near to the Losser city (source: <https://www.youtube.com/watch?v=fdCfSIszd04>)

In spite of the winter period, the flood also occurred in April and August 2015 following extreme rainfall events. The flood occurred at this time (April 1, April 4 and April 6) was flooded 111.49 ha, 103.67 ha and 27.36 ha of lands, respectively. On August 19, 2015, an area of 33 has were flooded. Very small flood was also observed on September 28, 2016, which was flooded 9 ha of land. Figure 14 shows the number of Sentinel-1 images observed as flood image from the analysis of 50 images for Dinkel river. According to the analysis, February was observed as the most flooded month and also when the peak flood occurred.

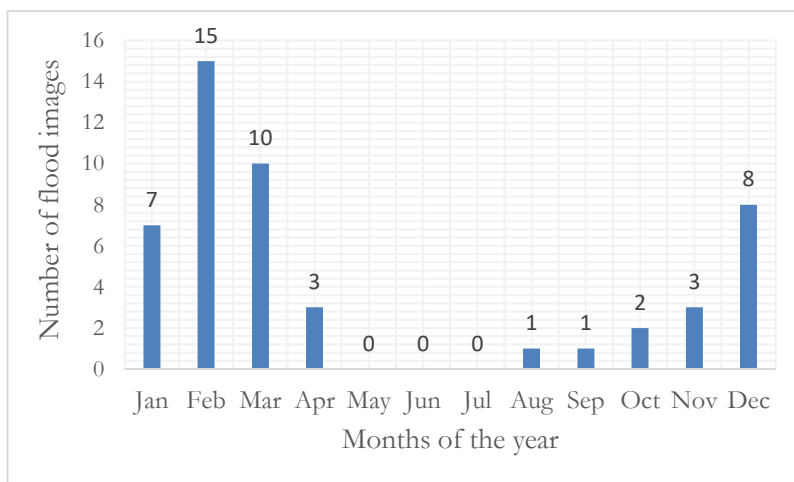


Figure 14: Number of the time-series Sentinel-1 SAR images observed as the flood for each month of the year starting from October 2014 to March 2017, to indicate which months are usually flooded

#### 5.4.2. Retention reservoirs time series flood maps

A shapefile of the reservoirs, provided by the regional water authority was overlay with Sentinel-1 images in order to analyse the flood extent. However, it was observed that flood detection over small reservoirs is not possible with the Sentinel-1 resolution. Hence, five retention reservoirs having an area of more than one hectare and in-situ water level measurements were selected. The subset was done for all retention reservoirs in order to assess each of them individually. One of the main reasons of subset was to set the threshold values. It was observed that setting the threshold value for the whole images is not effective and leads to misclassification. Hence, it was considered that better to set the threshold values for each subset individually.

According to the time series assessment, most of the retention reservoirs were observed as not completely flooded. This possibly depends on the conditions of the magnitude of the flood need to be diverted into the retention reservoir. In principle, retention reservoirs are designed to retain flood water, which occurs during extreme flood events. This means retention reservoirs are not observed with the water all the time as permanent water bodies like lakes and ponds. Hence, detection of water pixels over the reservoirs from remote sensing imagery is only done for a flooded date. However, diverted flood water after the storm may stay for some time based on the interest of water managers from a management point of view. In such case, water pixel will also detect. If the flooded water may contain debris and farmland residue on its surface, the amount of backscatter value will increase because of diffuse backscattering which leads to misclassification of flood pixels as non-flooded pixels. Compared to Dinkel river, retention reservoirs are situated on free open space. This condition minimizes the wrong classification that may happen due to undesirable objects like trees and submerged vegetation found at the edge of reservoirs.

The surface area of the flood was calculated to the extent of each reservoirs polygons. Hence, here it is presented in the form of percentage to their total area. All retention reservoirs studied here were gets flooded by less than 40 % of their total area except that of OV0002 retention reservoir. Time series flood maps on Figure 15 shown that OV0002 retention reservoir was flooded to its full capacity during February 12, 2016, compared to the other dates. At this date, 97 % of the reservoir area was getting flooded which covered an area of 4.13 ha. This flood was happened because of highly increased water level beyond the capacity of Vecht river. The extent of the flood on this date was going beyond the boundary of retention reservoir. The water level was raised from an approximate normal water level of 1 m to 1.97 m which mean almost doubled its depth. The second, third and fourth high flooded date recorded for OV0002 occurred during December 02, 2015, February 24, 2016, and January 24, 2015, which flooded 90 %, 84 % and 73 % of the total reservoir area, respectively. For the rest of the time, the spatial distribution of the flood was observed relatively very less because river banks can hold income discharge, and the reservoirs are not used or only to a small extent.

The multi-temporal flood map assessment shows that there is the almost uniform spatial distribution of flood extents based on different time and location where covered by the floods. However, in case of the HV0001, the pattern of the flood is not likely the same over a different period. This could be possible happened because this reservoir is surrounded by three water bodies from North, East and South-West part. Therefore, either of these water bodies become flooded at a different position and different time may result in the non-uniform distribution of flood extents. The time series flood maps for HV0001, OK0302, and SZ0265 are available in Appendix C.

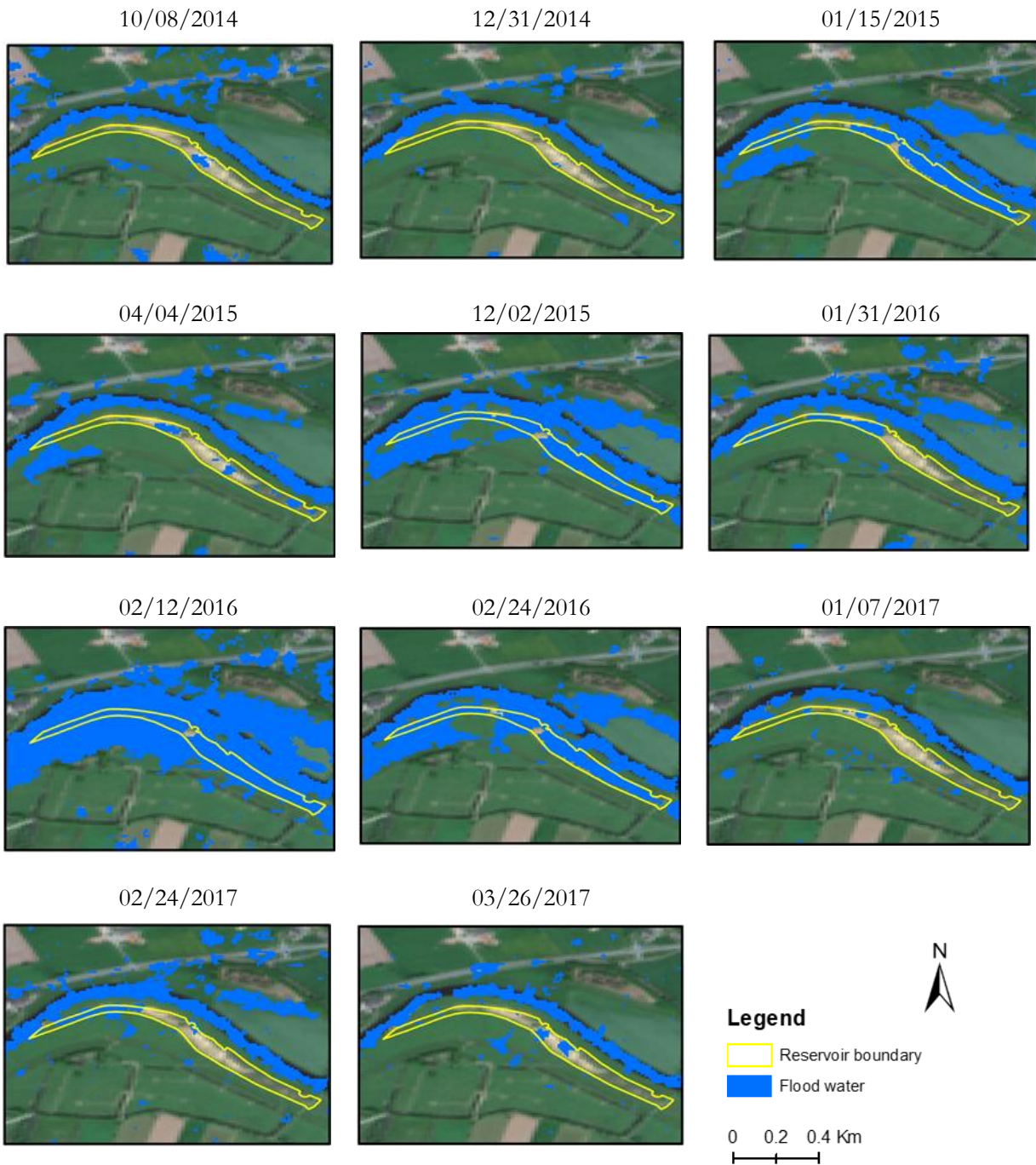


Figure 15: OV0002 retention reservoir time series flood map (November 08, 2014 to March 26, 2017). The place observed as a flood for every image is the part of Vecht river, and the yellow line indicates the location of OV0002 retention reservoir

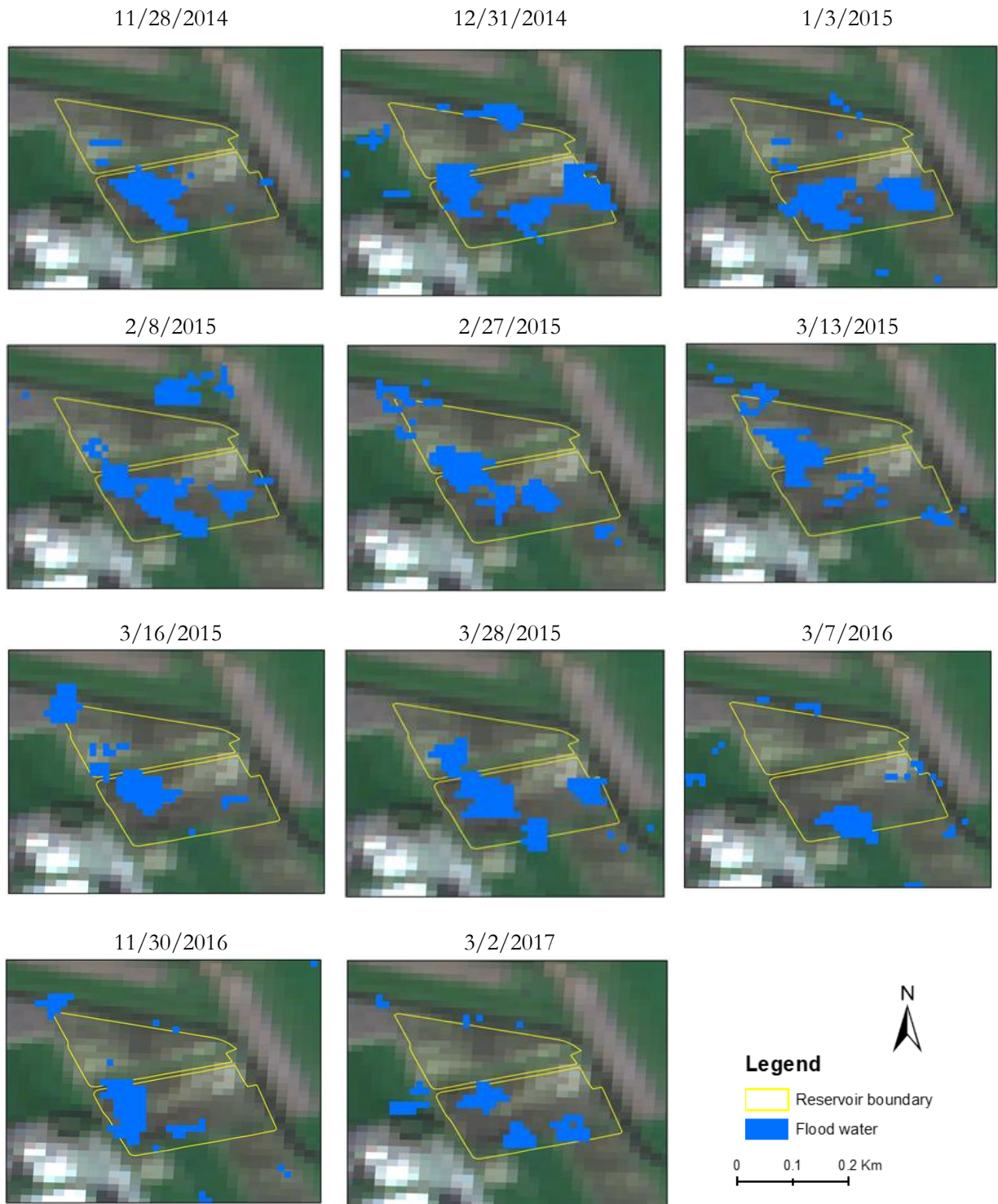


Figure 16: DV0277 retention reservoir time series flood map (November 28, 2014, to March 2, 2017)

## **5.5. Flood frequency maps**

In the previous sections, the multi-temporal data obtained from Sentinel-1 SAR imagery were used for generation of time series flood maps showing a spatial and temporal variation of flood extents. The development of flood frequency map is very important to identify which parts of the river and reservoir areas are most frequently gets flooded. Based upon this information, respective water managers can take the required management measures. This section present the flood frequency map shows how often each pixel flooded. For the development of the flood frequency maps, ArcGIS spatial analyst tool was used.

### **5.5.1. Dinkel river**

In the case of the Dinkel river, fifty images were used for generating flood frequency map; the result is shown in Figure 17. The deep blue colour on the right side of Figure 17 indicates that the permanent water bodies (lakes) detected in every Sentinel-1 time series images during both dry and wet periods. Those deep blue colours mapped along the Dinkel rivers indicates the most frequently flooded areas. From a management point of view, those areas are required great attention. According to the available information, farmers within Dinkel catchment can gain compensation per frequency by which their lands become flooded. Therefore, the frequency map provides the information to both farmers and water managers in order to maintain conflict free agreement based upon pre-defined rules and regulations.

### **5.5.2. Retention reservoirs**

Regarding the retention reservoirs, flood frequency maps (Figure 18), each reservoirs flood frequency maps having a different number of images and also different intervals were developed. WDO Delta water managers can be benefitted from the developed flood frequency maps for their operational water management. Compared to HV0001 and OV0002, the rest of three reservoirs are small in the size. For most of the SAR images, retention reservoirs were observed as dry (no flood). The position of each reservoir was evenly distributed over the specified study area. Hence, not all reservoirs are equally getting flooded on the same date. Finally, this is results on a different date of Sentinel image (see Appendix B), and as a consequence different frequency intervals. The condition of the flood of each reservoir depends on the magnitude of the flood. If the high magnitude of the flood is expected it will be diverted into the retention reservoirs. Most probably, an overestimation of flood extent may occur for SZ0265 reservoirs for one or two images. It is why more pixels observed as flood outside the extent. In the case of OV0002, deep blue colour indicates the Vecht river that observed in all Sentinel-1 images.

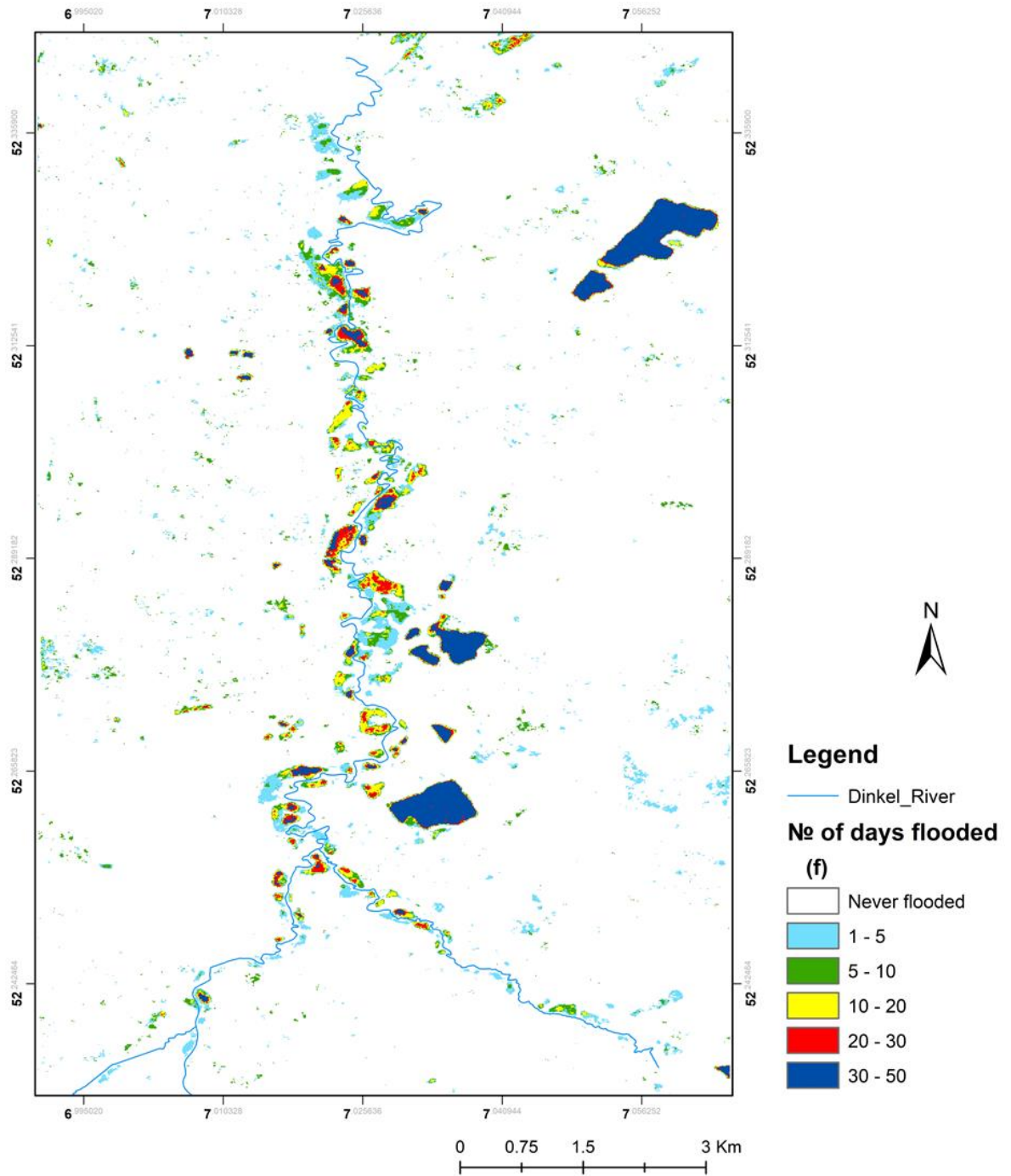


Figure 17: Flood frequency map for Dinkel river developed from the combination of flood maps between December 14, 2014, and March 11, 2017

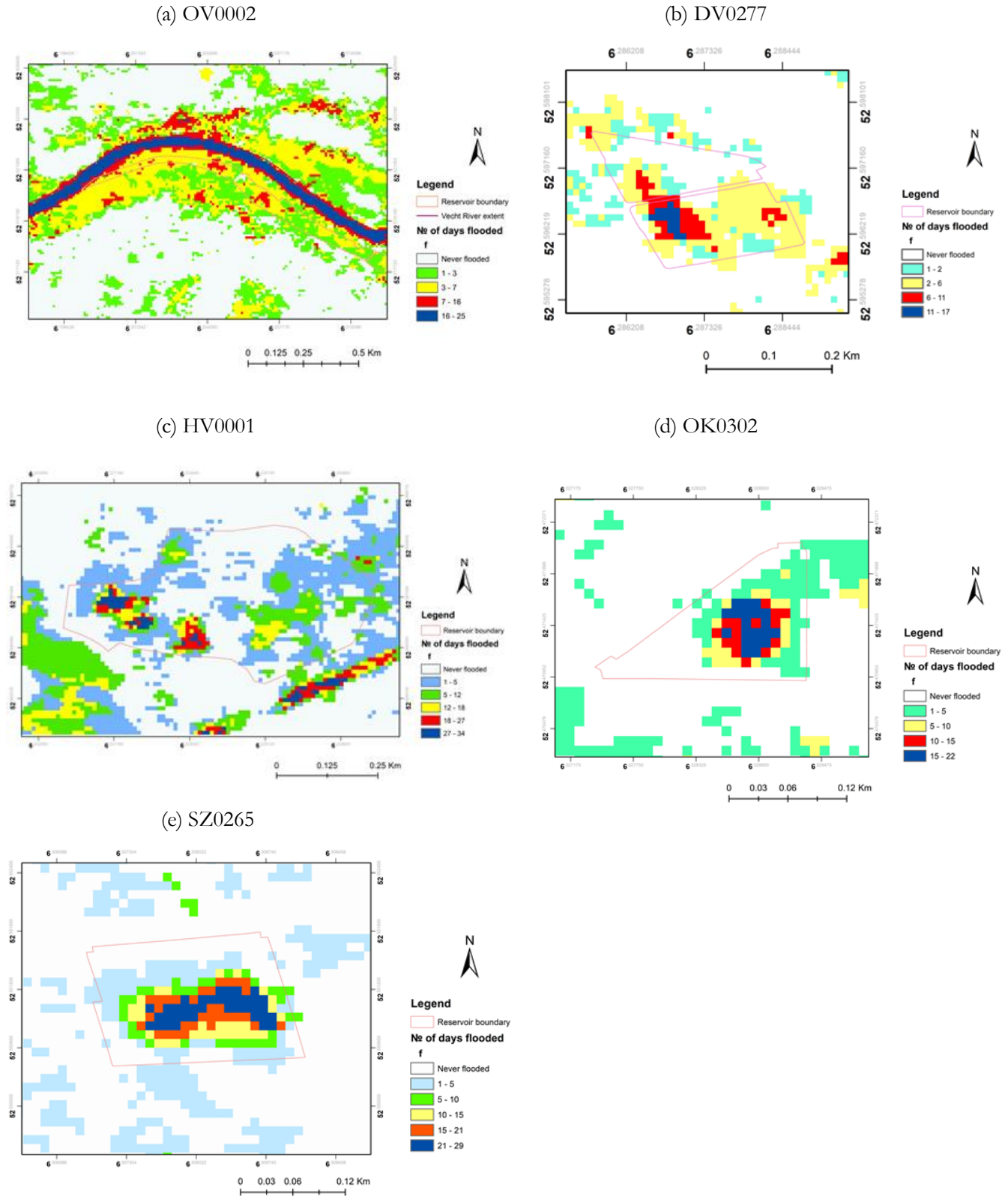


Figure 18: Flood frequency maps developed for retention reservoirs from the flood maps between October 08, 2014 to March 26, 2017

### 5.6. Water level estimation from flood maps and digital elevation model

Estimation of surface water level was done by combining extracted flood map with the DEM that is described in section 3.2.2. The accuracy of water surface level obtained from such kind of approach is highly influenced by the accuracy of retrieved flood extent and DEM resolution (Grimaldi et al., 2016). Comparison of the results of in-situ measured water levels and Sentinel-1 SAR derived water levels done for this study are discussed in subsequent section. Generally, the surface water levels estimated for the Dinkel river (Figure 19) showed a good agreement with the ground truth (in-situ measured) in compare to the water levels estimated for retention reservoirs. Figure 19 shows a sample of merged/combined DEM with the flood extent map on February 10, 2016. The same procedure was applied for the other flood maps in order to estimate the water levels.

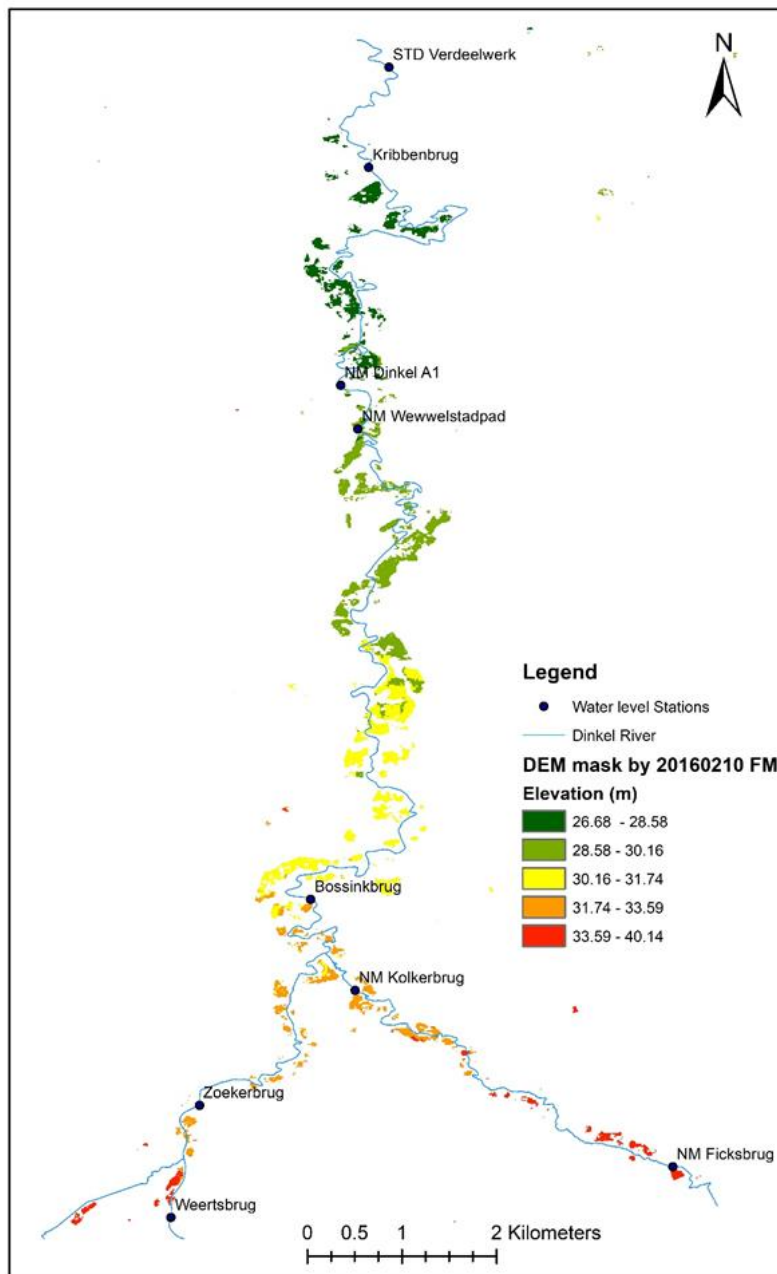


Figure 19: Water level estimation from flood map (February 10, 2016) merged with DEM for Dinkel river

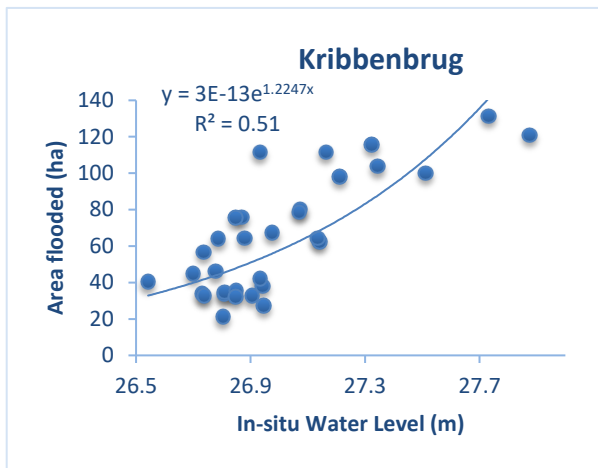
From the inspection of time series flood maps, it was observed that the stations such as Verdeelwerk, Weertsbrug and Ficksbrug were not usually experienced the floods. Hence, they were not used for the estimation of water levels in order to compare with in-situ measured water levels.

### **5.7. Flood extent vs. in-situ measured water levels**

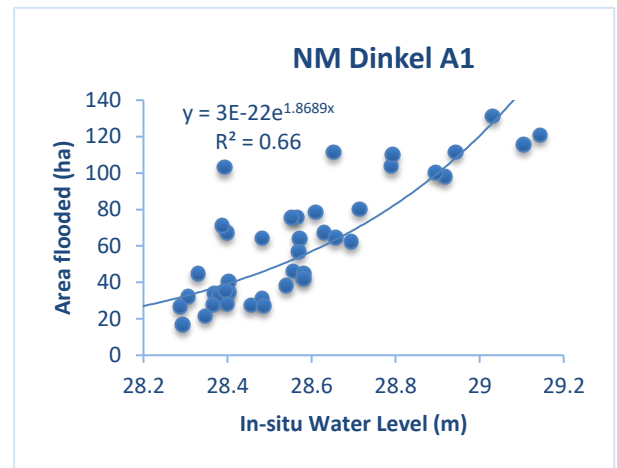
In order to examine the relationship between time series flood extent maps developed from Sentinel-1 SAR and the in-situ measured water levels, surface area of the flood extent was calculated for all flood maps. Then, the relationship between in-situ measured water levels and flood surface area was determined by means of ( $R^2$ ) (Mahe et al., 2011). The flooded surface areas for Dinkel river were calculated within 400 m buffering to the Dinkel river (line) digitized from google earth. From the multi-temporal images, it was recognized that some part of the permanent water body is within this buffering zone. Hence, those permanent water bodies (lake) were deducted from the calculation of total area in order to remain with the flooded area only. The assessment of flood extent shown that maximum flooded area was obtained for February 24, 2016, which covered an area of 131 hectares.

According to the available data, the water level measurements recorded at this date is the second highest water level recorded within this study period. In spite of more area gets flooded on February 24, 2016, the peak water level was recorded at all stations along Dinkel river on December 02, 2015 which flooded 120.93 ha of land. Most probably such uncertainty between water level and the area flooded was maybe happened because of flood water delay or misclassification of the non-flooded area as a flooded area. The lowest area of the flood, 17.18 ha was calculated for January 16, 2017, when the lowest water level measurement was recorded as well. The correlation analysis showed that Bossinkbrug station has the high relationship between area flooded area and in-situ water level with the  $R^2$  value of 0.91 (see Figure 20). This station shows better agreement between Sentinel-1 derived and in-situ measured water level.

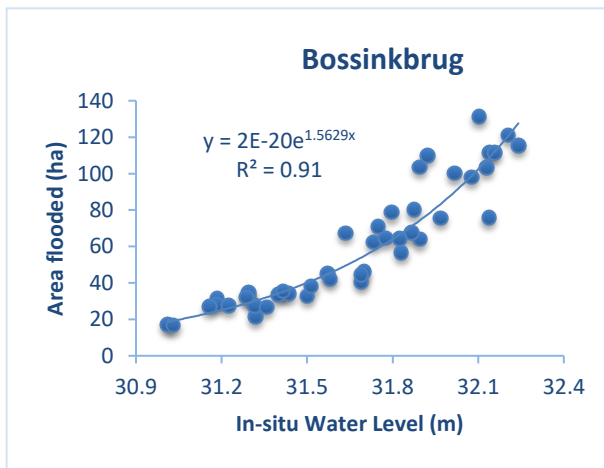
However, Kribbenbrug (Figure 20) gives poor correlation result compare to the other stations along the Dinkel river. In the previous assessment, the comparison of water levels between in-situ and Sentinel-1 at this station also provided low correlation. This is mainly because the uncertainty observed for flood map was propagated into water level estimation. Because, we have used the flood extent map for the estimation of the water level. Usually, Ficksbrug station was not getting a flood, hence we did not use for water level estimation in next (section 3.2.2). But here it is possible to consider since the flood surface area is calculated all over the flooded pixels. The others Dinkel river water level measurement stations were shown satisfactory correlation results. From the non-linear relationship between surface area of the floods and water levels we recognize that, as the water level gets increase and increase, more area becomes flooded with a small increase in water levels. We can observe this issue from Figure 20 (d) for Dinkel river at Bossinkbrug station.



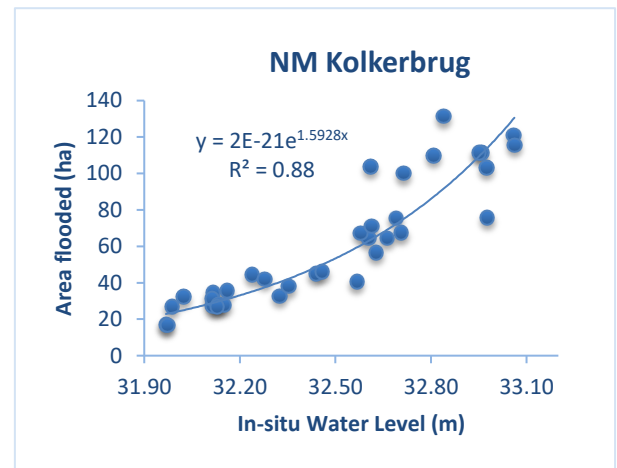
(a)



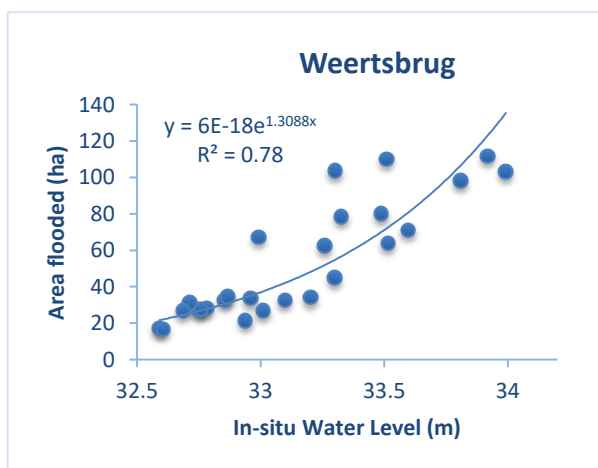
(b)



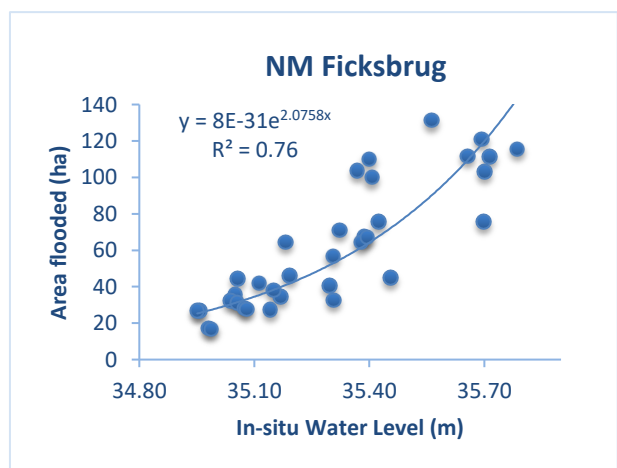
(c)



(d)



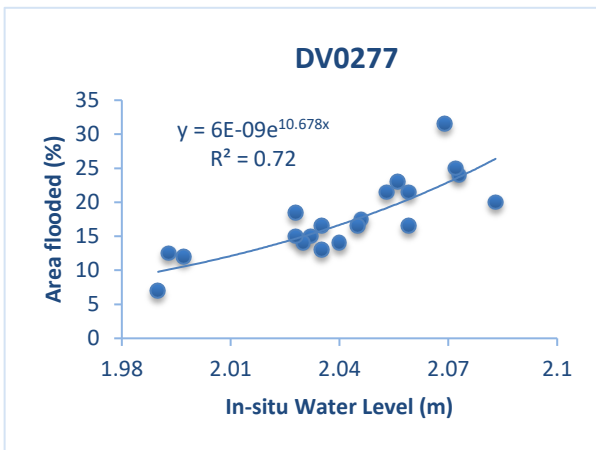
(e)



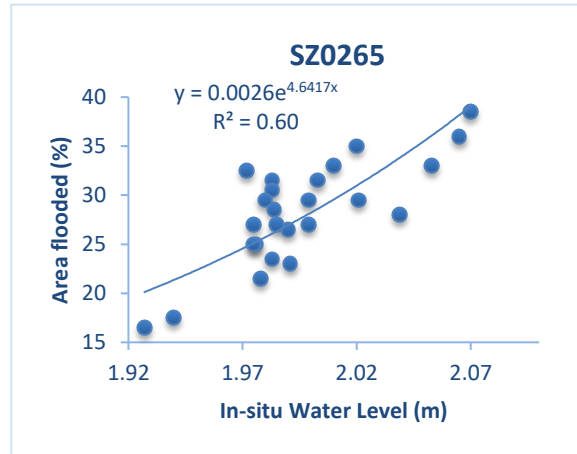
(f)

Figure 20: Comparison of flood surface area with in-situ measured water lever for Dinkel river

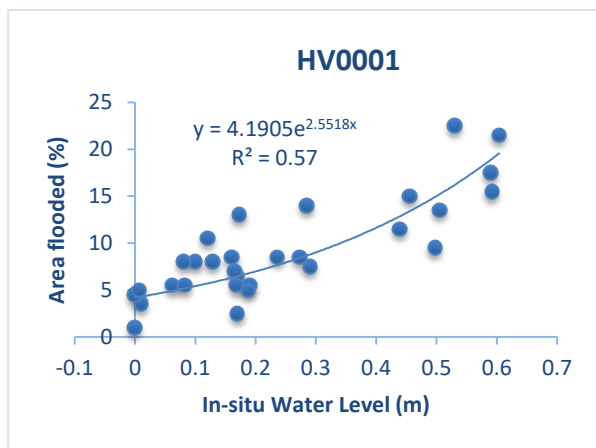
In the case of flood retention reservoirs, flood surface area was calculated to the extent of each reservoir boundary and presented as a percentage. Except for OV0002 reservoir (Figure 21, d) flooded up to 97 % during February 12, 2016, the rest of reservoirs were flooded less than 40 % of their total area. The correlation results obtained over retention reservoirs were also observed relatively low. As mentioned in the previous section, flood delay in the reservoir after high or low in-situ water level measurement may be one of the main cases why low correlation was obtained. Uncertainty may happen during flood extent extraction by using thresholding method is also the other case contribute to this variations as well. The correlation results obtained for each reservoir was presented here below.



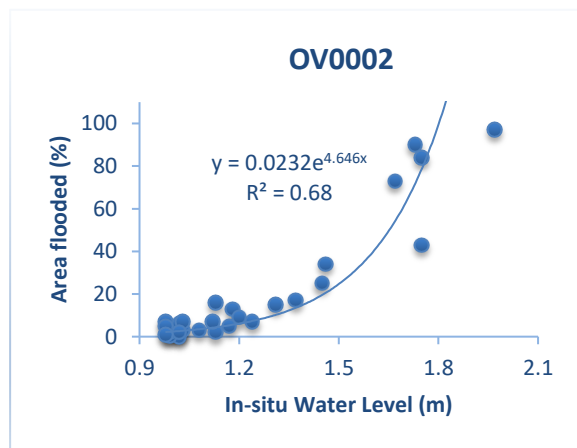
(a)



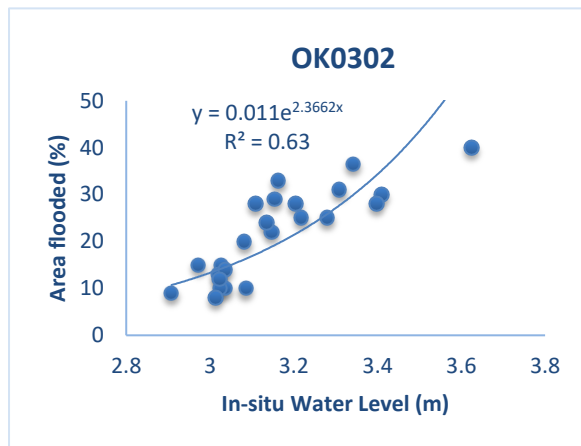
(b)



(c)



(d)



(e)

Figure 21: Comparison of flood surface area with in-situ measured water level for retention reservoirs

### 5.8. Sentinel-1 derived water levels vs. in-situ measured water levels

The water surface levels derived from merging Sentinel-1 SAR flood extent maps with DEM was tested for its reliability with the ground truth (in-situ water levels). For the comparison, in-situ water level recorded at the same time as Sentinel-1 pass was used. For most of the stations, high temporal resolution up to 15 minutes is available. The rest of stations have a measurement at hourly intervals. Sentinel-1 has three constant pass time over the study areas at 5:49, 17:16 and 17:24.

In order to evaluate the performance of Sentinel-1 derived water levels, root mean square error (RMSE) and bias (mean error, ME) were used. The coefficient of determination ( $R^2$ ) between Sentinel-1 derived, and the in-situ measured water level was also determined. There is one limitation of using bias. As the positive and negative differences are incorporated in the analysis, they cancel out each other and result in small difference (errors). However, RMSE is free from such limitation since it uses the squared difference. Figure 22 shows the linear correlation obtained for five stations over Dinkel and Figure 22 for retention reservoirs. The evaluation results show that water surface levels estimated for Dinkel river is agreed with the in-situ measured water level. Generally, poor performance evaluation value was obtained for retention reservoirs. This is because of the position of the in-situ water level measurements is far away from the place where flooded pixels were detected.

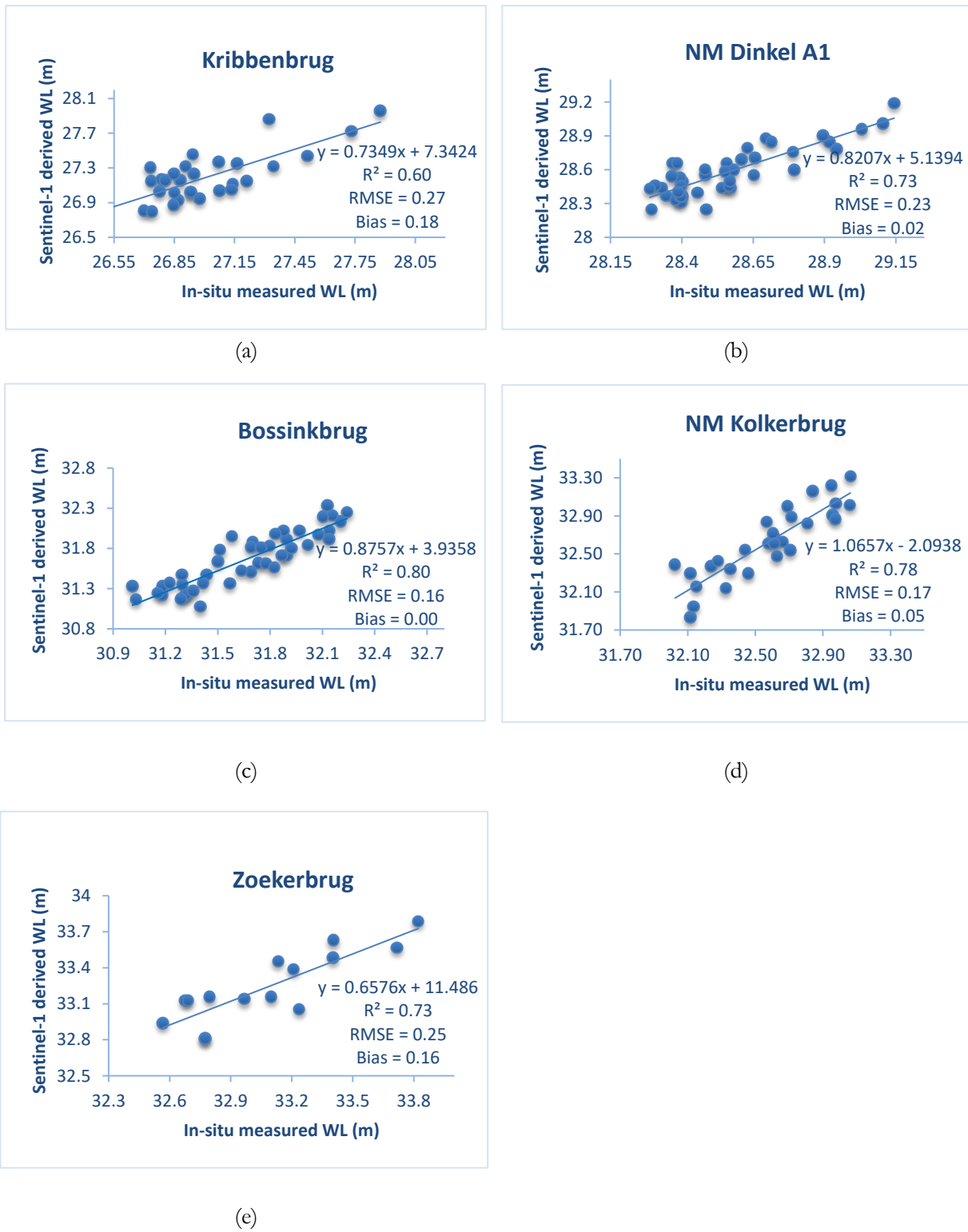


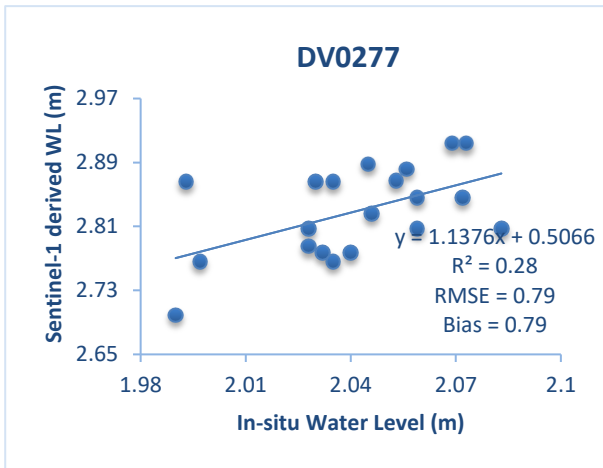
Figure 22: Correlation results between Sentinel-1 derived and in-situ measured water level for Dinkel river

The comparison of in-situ versus Sentinel-1 retrieved water levels for Dinkel river shown that the lowest r-square value ( $R^2 = 0.60$ ) is obtained for Kribbenbrug station (Figure 22, a) RMSE and bias for this station were also observed higher than the other stations with the value of 0.27 m and  $-0.18$  m, respectively. Kribbenbrug was not frequently getting flooded as the other stations. The location where flood occurs is not close to Kribbenbrug measurement station for most of the images. This explains the low correlation between in-situ measured and Sentinel-1 derived water level for this station. In the case of other stations, good correlation results were obtained and lower RMSE values. Among the other stations, Bossinkbrug has the highest correlation,  $R^2$  of 0.80, RMSE of 0.16 m and bias of  $-0.002$ . We cannot conclude the performance assessment based on only bias calculation because positive and negative differences cancel out each other and result in small bias. However, RMSE is considered as best performance measure since it squared difference. Within this study, the lowest (RMSE = 0.16) was obtained for Bossinkbrug water level measurement station.

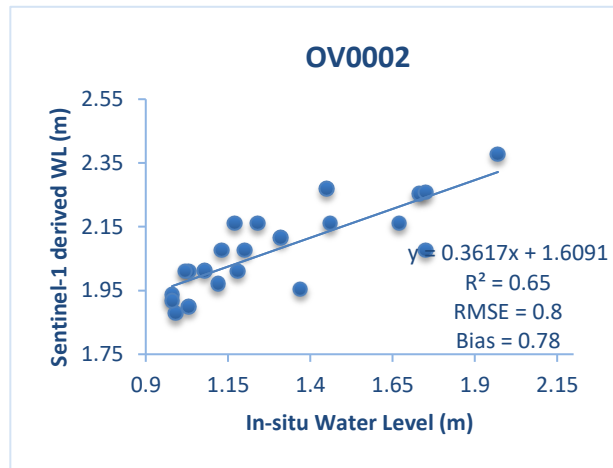
In general, almost all of the stations except Kribbenbrug, shown good agreement with ground truth with  $R^2 > 0.72$  and RMSE values are in the range of 16 to 27 cm. In comparison to the previous studies, the result obtained here is satisfactory. The study for Alzette river, Luxembourg using ENVISAT ASAR provide RMSE of 41 cm (Matgen et al., 2007). Recently, the study over six Canadian lakes by Nielsen et al. (2017) shown the RMSE range from 5 to 68 cm for CryoSat-2 and 17 to 54 cm for ENVISAT. They have used SAR Interferometer Radar Altimeter (SIRAL) for CryoSat-2 and Radar Altimeter 2 (RA-2) for ENVISAT. Compared to ENVISAT, Sentinel-1 SAR estimate the water level up to RMSE of 16 cm within this study.

In contrast to the performance of Sentinel-1 over Dinkel river mentioned above, poor performance results were obtained for retention reservoirs. This is not because of the inability of Sentinel-1 SAR to detect flood extent or because of the spatial resolution of DEM. However, it is most probably because of the position of gauging station and a place where the flood is detected. According to the available data, most of the reservoirs have not their measuring station. Therefore, nearby canals/river gauging stations were used. Hence, comparing in-situ water level with Sentinel-1 derived water levels was results on high variation. For instance, OK0302 shows error up to one meter, RMSE = 1.01 m. However, its linear statistics shows  $R^2 = 0.68$  (see Figure 23 d). This means even if there is variation in the measurement, they follow the same pattern, when the in-situ water level decrease, the water level from Sentinel-1 also decrease and vice versa. OV0001 retention reservoir is situated along the Vecht river. As far as the water levels getting high in the river, it will start to be diverted into the retention reservoirs. The water level estimated from the combination of Sentinel-1 and DEM are slightly higher than in-situ water levels. This is possibly happens because flood water delayed. Once high water level recorded on the river and then water was diverted into the reservoirs, the water level will be back to normal level (decrease after the storm). However, the diverted water may stay in the reservoir for some time without changing its level.

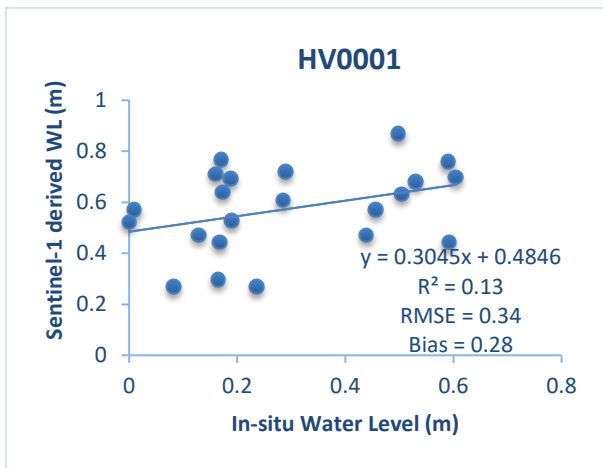
Furthermore, some reservoirs have very small variation in water level measurement, which is less than 10 cm (see, Figure 23, a). It is very difficult to match such fine accuracy with spaceborne satellite. The shape of the reservoir itself also affects the estimation water levels. If the shape of the reservoir is likely deeper and concave up, even if water level increase it is stored vertically upward and will not spread out. Under such case, remote sensing sensor will detect the same extent of flood over different time regardless of increase or decrease in water level. This possibly results in the variations of water levels.



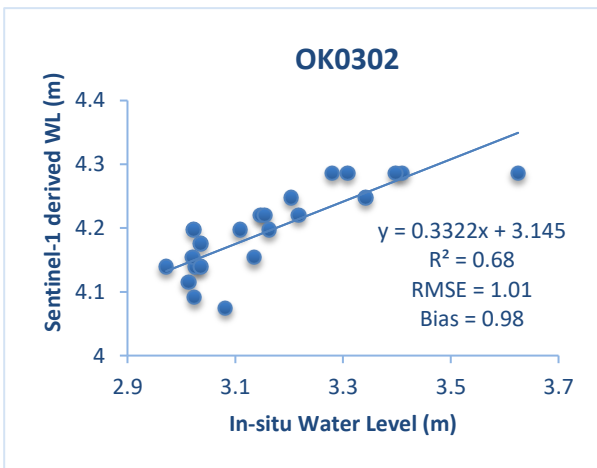
(a)



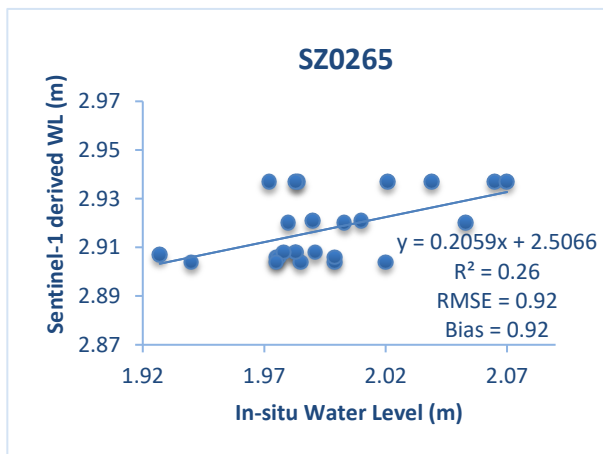
(b)



(c)



(d)



(e)

WL: water level

Figure 23: Correlation results between Sentinel-1 derived and in-situ measured water level for retention reservoirs

Table 5 summarizes the performance evaluation for both retention reservoirs and Dinkel river station performance evaluation. Almost the evaluation for RMSE and bias, also  $R^2$  follow the same pattern. However, we cannot say that very small bias value indicates high correlation since the positive and negative sign cancels each other. In the case of RMSE, we use the squared difference. Therefore it will not cancel each other. RMSE is considered as more trusted standard errors calculation than bias.

Table 5: Summary of performance assessment for both study areas

Stations name		Sentinel-1 derived water level vs. In-situ measured water level			Flooded surface area vs. In-situ measured WL
		$R^2$	RMSE (m)	Bias ( $\pm$ m)	$R^2$
Dinkel River	Kribbenbrug	0.599	0.268	0.182	0.515
	NM Dinkel A1	0.729	0.210	0.017	0.659
	Bossinkbrug	0.794	0.159	0.002	0.910
	NM Kolkerbrug	0.786	0.178	0.047	0.882
	Zoekerbrug	0.728	0.252	0.158	0.508
R. Reservoirs	DV0277	0.279	0.789	0.787	0.719
	HV0001	0.131	0.345	0.280	0.571
	OK0302	0.683	1.012	0.984	0.640
	OV0001	0.657	0.805	0.779	0.685
	SZ0265	0.264	0.922	0.921	0.600

## 6. CONCLUSION

This study investigated the capability of multi-temporal Sentinel-1 SAR data for the generation of time series flood maps and water levels estimation with the combination of the high-resolution digital elevation model (DEM). Within recent years, remote sensing and earth observation approaches have become a vital information source for monitoring of surface water dynamics. In fact that, floodwater is associated with high rainfall and cloudy conditions under which optical and thermal remote sensing techniques do not provide the data about the flood. However, the Synthetic Aperture Radar (SAR) mounted on Sentinel-1 satellite offers the possibility to acquire high-resolution images under all weather conditions and at any time. Of the VH/VV dual polarization of Sentinel-1, VV polarization was provided the better possibility to discriminate water body from other land surfaces. Therefore, multi-temporal SAR images in VV polarization collected within interferometric wide swath (IW) mode was used for this study.

SAR images are inherently degraded by speckle noise. This effect was reduced by applying Refined Lee speckle filtering using SNAP toolbox. It is selected based on its capability to suppress the speckles and at the same time preserves the edges details compare to the other filtering mechanisms. Based on literature reviews, delineation of flooded extent was done through global thresholding approach. The analysis of time series data shows that not only single threshold value works efficiently for all images. Therefore, the threshold values within the interval of -18 dB to -14 dB were applied for extraction of the flood extents. Three class of threshold values were applied for all images at first, then by critically looking at the images visually, adjustment of threshold has done for those need adjustment. In the case of water level estimation, an indirect method was adopted. Subsequently, the time series flood extent maps results were integrated with DEM to the estimate water levels. It is realized that the uncertainties may happen in the flood extent maps can be propagated into the water level estimations. To verify the reliability of the flood inundation, the comparison of flooded area with in-situ water level has done in addition to water levels comparisons. The results obtained for the flooded area vs. in-situ water levels were better than the results gained for Sentinel-1 and in-situ water level measurements. This indicates that there may be uncertainties occurs due to an approach of estimating water levels through merging flood extent maps with DEM.

The results of this study emphasized that the effectiveness of Sentinel-1 SAR was more reliable for the Dinkel river than the retention reservoirs when it is compared with in-situ data. The water levels estimated from Sentinel-1 was also correlated with in-situ water levels. The results show that high correlations were obtained for the Dinkel river at Bossinkbrug station. At this station, the root mean square error (RMSE) of 16 cm and an  $R^2$  value of 0.80 was obtained. Generally, the lowest correlation results were recorded for the retention reservoirs. This is mainly because of the difference between the positions of in-situ water level measurement and where flooded pixels were detected. For retention reservoirs, HV0001 provided the lowest  $R^2$  value of 0.13 in this study. For some of the retention reservoirs, the in-situ water level measurement is varied by very few cm, which is a bit difficult to quantify from the Sentinel-1 observations. This also possibly results in low correlation results.

In general, this study showed that Sentinel-1 SAR products could be used for monitoring of reservoir water levels and flooding of the river. In comparison to the previous studies done with the sensors like ENVISAT-ASAR, Sentinel-1 was provided a satisfactory result within this study. Therefore, the water management authorities can use the information obtained from this study for their management practices and they can also conduct further study themselves using Sentinel-1. In order to give insight on the parts of the river and retention reservoirs that most frequently flooded, flood frequency maps were developed from multi-temporal images. According to the assessment of flood maps, more images with peak flood events were detected in the winter season. This is important information for the water managers to develop the alternative way of flood mitigation measures in advance and assess the damage.

## 7. LIMITATIONS AND RECOMMENDATIONS

### 7.1. Limitations

For this study, many multi-temporal Sentinel-1 SAR images have been used. Hence, processing of those multi-temporal images consumed a considerable amount of time. So, it was not possible to apply alternative ways of extraction of the flood extent from the images and compare their results. Nevertheless, the methods used here for flood mapping and water level estimation were observed satisfactory. Here, some possible sources of uncertainty and limitations of this study are identified.

Start from pre-processing of the image; we may have introduced errors when we selected the speckle filtering method. The effectiveness of the speckle filter to suppress the noise preserve spatial detail is not equal for all available methods. In our case, we have selected the Refined Lee method. Even if this method was considered as an appropriate speckle filter, one of its main problems is its used fixed window 7x7 in SNAP. It is not possible to adjust the size of the kernel. Hence, this may affect the accuracy of image classification.

Regarding the flood extraction, the flood mapping is less accurate when there is low contrast between water and non-water bodies. Backscatter signals will increase if the surface roughness of the water increases due to wind, rain or flooded vegetation. This will result in low contrast and lead to misclassification of water as non-water. In contrast to this, if the nearby land surface has very smooth roughness this will be possibly classified as water. It needs to define additional criterion above a certain backscatter value in order to facilitate additional class like flooded vegetation under some stable environmental conditions.

Selection of the threshold value highly influences the flood extent map. Since manual thresholding has been used, it is difficult to say that water pixels were perfectly extracted using binarization. Subjectiveness on the selection of threshold value could induce uncertainties in the generation of flood extent maps. The uncertainties occurred on flood map development propagates into the estimation of water levels, which is obtained from merging the flood map and DEM. It is possibly one of the main cases why some of the water levels derived from Sentinel-1 was not appropriately agreed with in-situ measured water levels.

Within this study, the difference between the position of in-situ water level measurement and where Sentinel-1 detected flood resulted in a low correlation with water level measurements. This issue has affected the judgment of the capability of Sentinel-1 for estimation of water level from flood extent maps and DEM. The DEM used for this study has no data over water bodies. Hence, it influenced the exact estimation of water levels. Furthermore, the resolution of Sentinel-1 and the shape of reservoirs and river also influence the accuracy of the water level estimations to some extent.

## 7.2. Recommendations

Based on the findings of this research study, the following recommendations and/or suggestions can be made for further study:

- Developing automated flood extent extraction approach is significant for multi-temporal flood extent mapping to facilitate monitoring in near-real-time.
- It is also better to consider the way to discriminate flood water from flooded vegetations since their backscatter values can differ.
- To reduce the uncertainties that may happen during the comparison or validation of estimated water levels obtained through merging flood extent map and digital elevation model, it is recommendable to have the in-situ measurement that represents the specific location under consideration.
- Since there is high spatial resolution DEM available for the whole Netherlands, one may use high spatial resolution data which is higher than that of Sentinel-1, like TerraSAR-X. Acquisition of optical images from Sentinel-2 or other optical sensors can also be used for the comparison of the flood maps with Sentinel-1 SAR.
- The Sentinel-1 flood maps have the potential to be integrated with 1D or 2D hydraulic and hydrologic flood models, like HEC-RAS, SOBEK, MIKE FLOOD and LISFLOOD to improve their predictive capabilities.

## LIST OF REFERENCES

---

- Alsdorf, D. E., Rodriguez, E., & Lettenmaier, D. P. (2007). Measuring surface water from space. *Reviews of Geophysics*, 45(2), 1–24. <https://doi.org/10.1029/2006RG000197>
- Barreto, T. L. M., Almeida, J., & Cappabianco, F. A. M. (2016). Estimating accurate water levels for rivers and reservoirs by using SAR products: A multitemporal analysis. *Pattern Recognition Letters*, 83, 224–233. <https://doi.org/10.1016/j.patrec.2016.05.015>
- Bayanudin, A. A., & Jatmiko, R. H. (2016). Orthorectification of Sentinel-1 SAR (Synthetic Aperture Radar) Data in Some Parts of South-eastern Sulawesi Using Sentinel-1 Toolbox. *IOP Conference Series: Earth and Environmental Science*, 47(1). <https://doi.org/10.1088/1755-1315/47/1/012007>
- Brisco, B., Touzi, R., van der Sanden, J. J., Charbonneau, F., Pultz, T. J., & D'Iorio, M. (2008). Water resource applications with RADARSAT-2 – a preview. *International Journal of Digital Earth*, 1(1), 130–147. <https://doi.org/10.1080/17538940701782577>
- Brown, K. M., Hambidge, C. H., & Brownett, J. M. (2016). Progress in operational flood mapping using satellite synthetic aperture radar (SAR) and airborne light detection and ranging (LiDAR) data. *Progress in Physical Geography*, 40(2), 196–214. <https://doi.org/10.1177/0309133316633570>
- Byun, Y., Han, Y., & Chae, T. (2015). Image Fusion-Based Change Detection for Flood Extent Extraction Using Bi-Temporal Very High-Resolution Satellite Images. *Remote Sens*, 7, 10347–10363. <https://doi.org/10.3390/rs70810347>
- Chini, M., Papastergios, A., Pulvirenti, L., Pierdicca, N., Matgen, P., & Parcharidis, I. (2016). SAR coherence and polarimetric information for improving flood mapping. *International Geoscience and Remote Sensing Symposium (IGARSS), 2016–Novem*, 7577–7580. <https://doi.org/10.1109/IGARSS.2016.7730976>
- Clement, M. A., Kilsby, C. G., & Moore, P. (2017). Multi-temporal synthetic aperture radar flood mapping using change detection. *Journal of Flood Risk Management*, 1–17. <https://doi.org/10.1111/jfr3.12303>
- Demir, V., & Kisi, O. (2016). Flood Hazard Mapping by Using Geographic Information System and Hydraulic Model: Mert River, Samsun, Turkey. *Advances in Meteorology*, 2016, 1–9. <https://doi.org/10.1155/2016/4891015>
- DLR, G. (2013). A Tutorial on Synthetic Aperture Radar. <https://doi.org/10.1109/MGRS.2013.2248301>
- El-Zaart, A. (2015). Synthetic Aperture Radar Images Segmentation Using Minimum Cross - Entropy With Gamma Distribution. *Signal & Image Processing: An Int. Journal*, 6(4), 19–31. <https://doi.org/10.5121/sipij.2015.6402>
- Erlich, M., Begum, S., Stive, M. J. F., & Hall, J. W. (2007). Flood Risk Management in Europe. *Flood Risk Management in Europe*, 25(December), 43–60. <https://doi.org/10.1007/978-1-4020-4200-3>
- Gan, T. Y., Zunic, F., Kuo, C. C., & Strobl, T. (2012a). Flood mapping of danube river at romania using single and multi-date ERS2-SAR images. *International Journal of Applied Earth Observation and Geoinformation*, 18(1), 69–81. <https://doi.org/10.1016/j.jag.2012.01.012>
- Gan, T. Y., Zunic, F., Kuo, C. C., & Strobl, T. (2012b). Flood mapping of danube river at romania using single and multi-date ERS2-SAR images. *International Journal of Applied Earth Observation and Geoinformation*, 18(1), 69–81. <https://doi.org/10.1016/j.jag.2012.01.012>
- Giustarini, L., Hostache, R., Matgen, P., Schumann, G. J., Bates, P. D., & Mason, D. C. (2013). A Change Detection Approach to Flood Mapping in Urban Areas Using TerraSAR-X. *IEEE Transactions on Geoscience and Remote Sensing*, 51(4), 2417–2430. <https://doi.org/10.1109/TGRS.2012.2210901>
- Giustarini, L., Matgen, P., Hostache, R., Montanari, M., Plaza, D., Pauwels, V. R. N., ... Savenije, H. H. G. (2011). Assimilating SAR-derived water level data into a hydraulic model: A case study. *Hydrology and Earth System Sciences*, 15(7), 2349–2365. <https://doi.org/10.5194/hess-15-2349-2011>
- Grimaldi, S., Li, Y., Pauwels, V. R. N., & Walker, J. P. (2016). Remote Sensing-Derived Water Extent and Level to Constrain Hydraulic Flood Forecasting Models: Opportunities and Challenges. *Surveys in Geophysics*, 37(5), 977–1034. <https://doi.org/10.1007/s10712-016-9378-y>
- Henry, J.-B., Chastanet, P., Fellah, K., & Desnos, Y.-L. (2006). Envisat multi-polarized ASAR data for flood mapping. *International Journal of Remote Sensing*. <https://doi.org/10.1080/01431160500486724>
- Hostache, R., Matgen, P., Schumann, G., Puech, C., Hoffmann, L., & Pfister, L. (2009). Water Level

- 
- Estimation and Reduction of Hydraulic Model Calibration Uncertainties Using Satellite SAR Images of Floods. *IEEE Transactions on Geoscience and Remote Sensing*, 47(2), 431–441.  
<https://doi.org/10.1109/TGRS.2008.2008718>
- Hostache, R., Matgen, P., & Wagner, W. (2012). Change detection approaches for flood extent mapping: How to select the most adequate reference image from online archives? *International Journal of Applied Earth Observation and Geoinformation*, 19(1), 205–213. <https://doi.org/10.1016/j.jag.2012.05.003>
- Jongman, B., Koks, E. E., Husby, T. G., & Ward, P. J. (2014). Increasing flood exposure in the Netherlands: Implications for risk financing. *Natural Hazards and Earth System Sciences*, 14(5), 1245–1255. <https://doi.org/10.5194/nhess-14-1245-2014>
- Kaufmann, M., Van Doorn-Hoekveld, W., Gilissen, H. K., & Van Rijswijk, M. (2016). *Analysing and evaluating flood risk governance in the Netherlands. Drowning in safety ?*
- Lee, J. S., Jurkevich, L., Dewaele, P., Wambacq, P., & Oosterlinck, A. (1994). Speckle filtering of synthetic aperture radar images: A review. *Remote Sensing Reviews*, 8(4), 313–340.  
<https://doi.org/10.1080/02757259409532206>
- Lee, J. Sen, Wen, J. H., Ainsworth, T. L., Chen, K. S., & Chen, A. J. (2009). Improved sigma filter for speckle filtering of SAR imagery. *IEEE Transactions on Geoscience and Remote Sensing*, 47(1), 202–213.  
<https://doi.org/10.1109/TGRS.2008.2002881>
- Logan, T., & Facility, A. S. A. R. (1995). Terrain Correction of Synthetic Aperture Radar Imagery Using the Cray T3D, 268–274.
- Long, S., Fatoyinbo, T. E., & Policelli, F. (2014). Flood extent mapping for Namibia using change detection and thresholding with SAR. *Environmental Research Letters Environ. Res. Lett*, 9, 35002–9.  
<https://doi.org/10.1088/1748-9326/9/3/035002>
- Mahe, G., Orange, D., Mariko, A. ., & Bricquet, J. P. (2011). Estimation of the flooded area of the Inner Delta of the River Niger in Mali by hydrological balance and satellite data. *LAHS-AISH Publication*, 344(July), 138–143. Retrieved from <http://www.scopus.com/inward/record.url?eid=2-s2.0-81755168950&partnerID=40&md5=ca83c4a2a186fb16f469f32b926151bc>
- Manjusree, P., Prasanna Kumar, L., Bhatt, C. M., Rao, G. S., & Bhanumurthy, V. (2012). Optimization of threshold ranges for rapid flood inundation mapping by evaluating backscatter profiles of high incidence angle SAR images. *International Journal of Disaster Risk Science*, 3(2), 113–122.  
<https://doi.org/10.1007/s13753-012-0011-5>
- Martinis, S. (2010). Automatic near real-time flood detection in high resolution X-band synthetic aperture radar satellite data using context-based classification on irregular graphs.
- Martinis, S., Kersten, J., & Twele, A. (2015). A fully automated TerraSAR-X based flood service. *ISPRS Journal of Photogrammetry and Remote Sensing*, 104, 203–212.  
<https://doi.org/10.1016/j.isprsjprs.2014.07.014>
- Martinis, S., Kuenzer, C., & Twele, A. (2015). Flood Studies Using Synthetic Aperture Radar Data. *Remote Sensing of Water Resources, Disasters, and Urban Studies*, 145–173. <https://doi.org/doi:10.1201/b19321-10>
- Matgen, P., Hostache, R., Schumann, G., Pfister, L., Hoffmann, L., & Savenije, H. H. G. (2011). Towards an automated SAR-based flood monitoring system: Lessons learned from two case studies. *Physics and Chemistry of the Earth*, 36(7–8), 241–252. <https://doi.org/10.1016/j.pce.2010.12.009>
- Matgen, P., Schumann, G., Henry, J. B., Hoffmann, L., & Pfister, L. (2007). Integration of SAR-derived river inundation areas, high-precision topographic data and a river flow model toward near real-time flood management. *International Journal of Applied Earth Observation and Geoinformation*, 9(3), 247–263.  
<https://doi.org/10.1016/j.jag.2006.03.003>
- McCandless, S. W., & Jackson, C. R. (2004). Chapter 1. Principles of Synthetic Aperture Radar. Retrieved from [http://www.sarusersmanual.com/ManualPDF/NOAASARManual\\_CH01\\_pg001-024.pdf](http://www.sarusersmanual.com/ManualPDF/NOAASARManual_CH01_pg001-024.pdf)
- Meenakshi, a V, & Punitham, V. (2011). Performance of Speckle Noise Reduction Filters on Active Radar and SAR Images. *International Journal of Technology And Engineering System (IJTES)*, 2(1), 111–114.
- Nielsen, K., Stenseng, L., Andersen, O. B., & Knudsen, P. (2017). The performance and potentials of the CryoSat-2 SAR and SARIn modes for lake level estimation. *Water (Switzerland)*, 9(6).  
<https://doi.org/10.3390/w9060374>
- Pham-Duc, B., Prigent, C., & Aires, F. (2017). Surface water monitoring within cambodia and the Vietnamese Mekong Delta over a year, with Sentinel-1 SAR observations. *Water (Switzerland)*, 9(6), 1–21. <https://doi.org/10.3390/w9060366>
- Potin, P. (2013). ESA Sentinel 1 handbook. *European Space Agency Technical Note*, 1–80.  
<https://doi.org/10.1017/CBO9781107415324.004>
- Pradhan, B., Hagemann, U., Shafapour Tehrany, M., & Prechtel, N. (2014). An easy to use ArcMap based

- texture analysis program for extraction of flooded areas from TerraSAR-X satellite image. *Computers and Geosciences*, 63, 34–43. <https://doi.org/10.1016/j.cageo.2013.10.011>
- Psomiadis, E. (2016). Flash flood area mapping utilising SENTINEL-1 radar data. <https://doi.org/10.1117/12.2241055>
- Qiu, F., Berglund, J., Jensen, J. R., Thakkar, P., & Ren, D. (2004). Speckle Noise Reduction in SAR Imagery Using a Local Adaptive Median Filter. *GIScience and Remote Sensing*, 41(3), 244–266. <https://doi.org/10.2747/1548-1603.41.3.244>
- radartutorial.eu. (n.d.). Radar Basics - Synthetic Aperture Radar. Retrieved November 26, 2017, from <http://www.radartutorial.eu/20.airborne/ab07.en.html>
- Santoro, M., & Wegmüller, U. (2014). Multi-temporal synthetic aperture radar metrics applied to map open water bodies. *IEEE Journal of Selected Topics in Applied Earth Observations and Remote Sensing*, 7(8), 3225–3238. <https://doi.org/10.1109/JSTARS.2013.2289301>
- Schlaflfer, S., Matgen, P., Hollaus, M., & Wagner, W. (2015a). Flood detection from multi-temporal SAR data using harmonic analysis and change detection. *International Journal of Applied Earth Observation and Geoinformation*, 38, 15–24. <https://doi.org/10.1016/j.jag.2014.12.001>
- Schlaflfer, S., Matgen, P., Hollaus, M., & Wagner, W. (2015b). Flood detection from multi-temporal SAR data using harmonic analysis and change detection. *International Journal of Applied Earth Observations and Geoinformation*, 38, 15–24. <https://doi.org/10.1016/j.jag.2014.12.001>
- Schumann, G., Bates, P. D., Horritt, M. S., Matgen, P., & Pappenberger, F. (2009). Progress in integration of remote sensing-derived flood extent and stage data and hydraulic models. *Reviews of Geophysics*, 47(3), 1–20. <https://doi.org/10.1029/2008RG000274>
- Sheng, Y., & Xia, Z. (1996). A comprehensive evaluation of filters for radar speckle suppression. *IGARSS '96. 1996 International Geoscience and Remote Sensing Symposium*, 1559–1561. <https://doi.org/10.1109/IGARSS.1996.516730>
- SMITH, L. C. (1997). Satellite remote sensing of river inundation area, stage, and discharge: a review. *Hydrological Processes*, 11(10), 1427–1439. [https://doi.org/10.1002/\(SICI\)1099-1085\(199708\)11:10<1427::AID-HYP473>3.0.CO;2-S](https://doi.org/10.1002/(SICI)1099-1085(199708)11:10<1427::AID-HYP473>3.0.CO;2-S)
- Torres, R., Snoeij, P., Geudtner, D., Bibby, D., Davidson, M., Attema, E., ... Rostan, F. (2012). GMES Sentinel-1 mission. *Remote Sensing of Environment*, 120, 9–24. <https://doi.org/10.1016/j.rse.2011.05.028>
- Tsyganskaya, V., Martinis, S., Twele, A., Cao, W., Schmitt, A., Marzahn, P., & Ludwig, R. (2016). A fuzzy logic-based approach for the detection of flooded vegetation by means of synthetic aperture radar data. *International Archives of the Photogrammetry, Remote Sensing and Spatial Information Sciences - ISPRS Archives*, 41(July), 371–378. <https://doi.org/10.5194/isprsarchives-XLI-B7-371-2016>
- Twele, A., Cao, W., Plank, S., & Martinis, S. (2016). Sentinel-1-based flood mapping: a fully automated processing chain. *International Journal of Remote Sensing*, 37(13), 2990–3004. <https://doi.org/10.1080/01431161.2016.1192304>
- Veci, L. (2015). SENTINEL-1 Toolbox SAR Basics Tutorial. Retrieved from [http://sentinel1.s3.amazonaws.com/docs/S1TBX\\_SAR\\_Basics\\_Tutorial.pdf](http://sentinel1.s3.amazonaws.com/docs/S1TBX_SAR_Basics_Tutorial.pdf)
- Westerhoff, R. S., Kleuskens, M. P. H., Winsemius, H. C., Huizinga, H. J., Brakenridge, G. R., & Bishop, C. (2013). Automated global water mapping based on wide-swath orbital synthetic-aperture radar. *Hydrology and Earth System Sciences*, 17(2), 651–663. <https://doi.org/10.5194/hess-17-651-2013>
- Yommy, A. S., Liu, R., & Wu, A. S. (2015). SAR image despeckling using refined lee filter. *Proceedings - 2015 7th International Conference on Intelligent Human-Machine Systems and Cybernetics, IHMSC 2015*, 2, 260–265. <https://doi.org/10.1109/IHMSC.2015.236>
- Zyl, van J. J., & Kim, Y. (2011). Synthetic Aperture Radars ( SAR ) Imaging Basics. *Synthetic Aperture Radar Polarimetry*, 334. Retrieved from [http://descanso.jpl.nasa.gov/SciTechBook/series2/02Chap1\\_110106\\_amf.pdf](http://descanso.jpl.nasa.gov/SciTechBook/series2/02Chap1_110106_amf.pdf)

# APPENDICES

---

## Appendix A: List of multi-temporal Sentinel-1 images

The image in VV-polarization mode was used for all flood extent extraction.

Sentinel-1 images naming convention used below: eg. S1A\_IW\_GRDH\_1SDV\_20141214\_05:41

(S1A: mission identifier, IW: mode, GRDH: product type and resolution class, 1SDV: processing level, Product class and Polarization, 20141214\_05:41 : start date/time in format of YYYYMMDD\_HHMM)

### A: Sentinel-1 mages used for Dinkel river

S.No	Sentinel-1 images	Pass	Track ID	Threshold value (dB)	Area flooded (ha)
1	S1A_IW_GRDH_1SDV_20141214_05:41	Descending	139	17.5	63.98
2	S1A_IW_GRDH_1SDV_20141219_05:49	Descending	37	14.5	34.06
3	S1A_IW_GRDH_1SDV_20141222_17:24	Ascending	88	16	62.40
4	S1A_IW_GRDH_1SDV_20141226_05:41	Descending	139	17	33.54
5	S1A_IW_GRDH_1SDV_20150115_17:24	Ascending	88	15.5	80.16
6	S1A_IW_GRDH_1SDV_20150119_05:41	Descending	139	16.5	32.76
7	S1A_IW_GRDH_1SDV_20150131_05:41	Descending	139	18	98.00
8	S1A_IW_GRDH_1SDV_20150203_17:16	Ascending	15	16	78.60
9	S1A_IW_GRDH_1SDV_20150224_05:41	Descending	139	16.5	21.40
10	S1A_IW_GRDH_1SDV_20150227_17:16	Ascending	15	15.1	44.85
11	S1A_IW_GRDH_1SDV_20150301_05:49	Descending	37	15.2	34.66
12	S1A_IW_GRDH_1SDV_20150304_17:24	Ascending	88	15.8	32.71
13	S1A_IW_GRDH_1SDV_20150401_05:41	Descending	139	16	111.50
14	S1A_IW_GRDH_1SDV_20150404_17:16	Ascending	15	15.5	103.67
15	S1A_IW_GRDH_1SDV_20150406_05:49	Descending	37	16	27.36
16	S1A_IW_GRDH_1SDV_20150819_17:24	Ascending	88	17	33.00 *
17	S1A_IW_GRDH_1SDV_20151118_17:16	Ascending	15	14.6	67.34
18	S1A_IW_GRDH_1SDV_20151120_05:49	Descending	37	15.5	38.05
19	S1A_IW_GRDH_1SDV_20151130_17:16	Ascending	15	15	75.71
20	S1A_IW_GRDH_1SDV_20151202_05:49	Descending	37	16.7	120.93
21	S1A_IW_GRDH_1SDV_20151205_17:24	Ascending	88	16.5	46.13
22	S1A_IW_GRDH_1SDV_20151212_17:16	Ascending	15	14.8	40.40
23	S1A_IW_GRDH_1SDV_20151214_05:49	Descending	37	16.5	56.71
24	S1A_IW_GRDH_1SDV_20160129_17:16	Ascending	15	15.5	44.54
25	S1A_IW_GRDH_1SDV_20160131_05:49	Descending	37	16.5	111.46
26	S1A_IW_GRDH_1SDV_20160203_17:24	Ascending	88	16.6	64.46
27	S1A_IW_GRDH_1SDV_20160207_05:41	Descending	139	16	35.53

28	S1A_IW_GRDH_1SDV_20160210_17:16	Ascending	15	17.3	115.47
29	S1A_IW_GRDH_1SDV_20160212_05:49	Descending	37	17.5	100.07
30	S1A_IW_GRDH_1SDV_20160215_17:24	Ascending	88	16.5	64.31
31	S1A_IW_GRDH_1SDV_20160224_05:49	Descending	37	17.4	131.25
32	S1A_IW_GRDH_1SDV_20160227_17:24	Ascending	88	16.3	32.13
33	S1A_IW_GRDH_1SDV_20160305_17:16	Ascending	15	16	75.48
34	S1A_IW_GRDH_1SDV_20160307_05:49	Descending	37	16.5	42.04
35	S1B_IW_GRDH_1SDV_20160928_05:41	Descending	139	18.2	9.50 *
36	S1B_IW_GRDH_1SDV_20161003_05:49	Descending	37	16.5	8.46 *
37	S1A_IW_GRDH_1SDV_20161012_17:24	Ascending	88	17.5	8.96 *
38	S1A_IW_GRDH_1SDV_20170101_05:49	Descending	37	16.5	5.79 *
39	S1A_IW_GRDH_1SDV_20170116_17:24	Ascending	88	17.5	17.18
40	S1A_IW_GRDH_1SDV_20170206_05:49	Descending	37	16	8.33 *
41	S1B_IW_GRDH_1SDV_20170224_05:49	Descending	37	16	103.08
42	S1A_IW_GRDH_1SDV_20170225_05:41	Descending	139	18.4	109.94
43	S1B_IW_GRDH_1SDV_20170227_17:24	Ascending	88	16	31.17
44	S1A_IW_GRDH_1SDV_20170228_17:16	Ascending	15	15	28.16
45	S1B_IW_GRDH_1SDV_20170303_05:40	Descending	139	17	67.21
46	S1A_IW_GRDH_1SDV_20170305_17:24	Ascending	88	16.5	27.61
47	S1B_IW_GRDH_1SDV_20170306_17:15	Ascending	15	15.5	16.72
48	S1B_IW_GRDH_1SDV_20170308_05:49	Descending	37	15.7	26.73
49	S1A_IW_GRDH_1SDV_20170309_05:41	Descending	139	16.1	71.01
50	S1B_IW_GRDH_1SDV_20170311_17:24	Ascending	88	17	26.97

Remark: \* Images not used for water level estimation

**B: Images used for retention reservoirs**

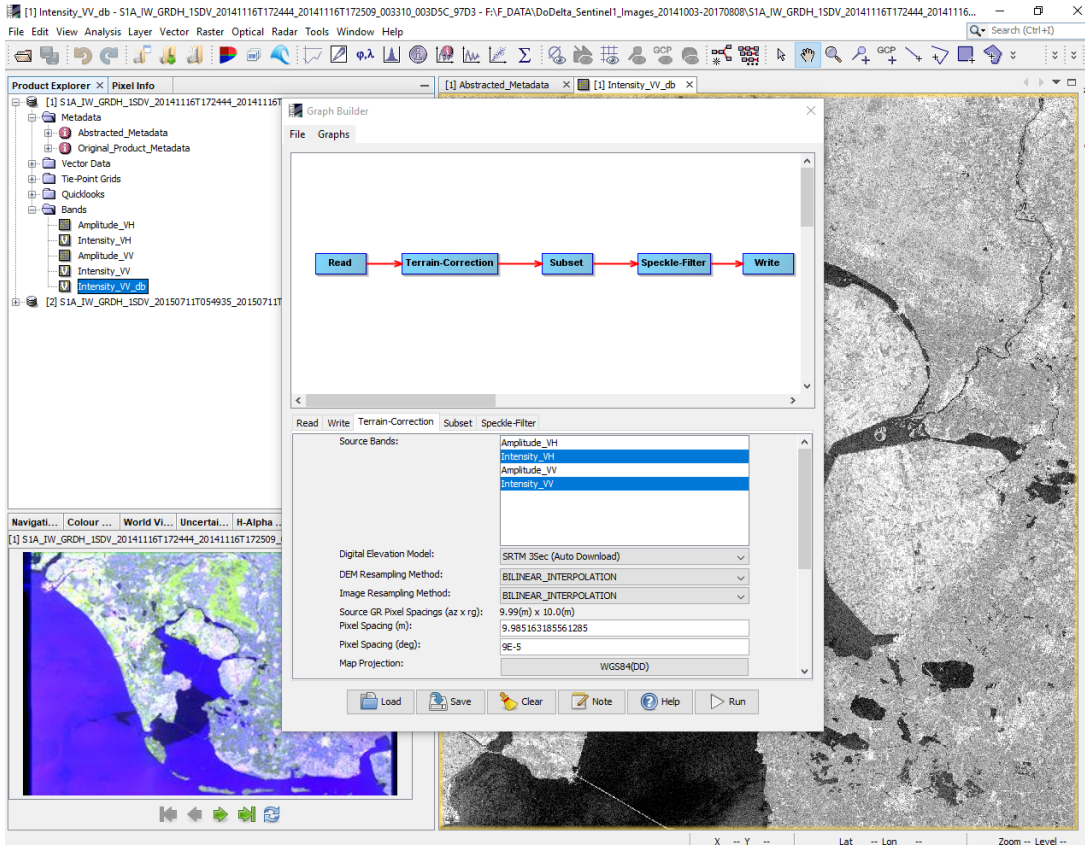
S.No	Sentinel-1 images	Pass	Track ID	Retention Reservoirs				
				DV0277	HV0001	OK0302	OV0002	SZ0265
1	S1A_IW_GRDH_1SDV_20141008_05:49	Descending	37		✓	✓	✓	
2	S1A_IW_GRDH_1SDV_20141116_17:24	Ascending	88					✓
3	S1A_IW_GRDH_1SDV_20141128_17:24	Ascending	88	✓	✓			
4	S1A_IW_GRDH_1SDV_20141219_05:49	Descending	37	✓	✓	✓	✓	✓
5	S1A_IW_GRDH_1SDV_20141222_17:24	Ascending	88		✓			
6	S1A_IW_GRDH_1SDV_20141231_05:49	Descending	37	✓			✓	✓
7	S1A_IW_GRDH_1SDV_20150103_17:24	Ascending	88	✓				
8	S1A_IW_GRDH_1SDV_20150115_17:24	Ascending	88	✓	✓		✓	✓
9	S1A_IW_GRDH_1SDV_20150203_17:16	Ascending	15		✓			
10	S1A_IW_GRDH_1SDV_20150205_05:49	Descending	37	✓			✓	
11	S1A_IW_GRDH_1SDV_20150208_17:24	Ascending	88	✓				
12	S1A_IW_GRDH_1SDV_20150217_05:49	Descending	37				✓	
13	S1A_IW_GRDH_1SDV_20150227_17:16	Ascending	15	✓	✓			
14	S1A_IW_GRDH_1SDV_20150301_05:49	Descending	37	✓	✓			
15	S1A_IW_GRDH_1SDV_20150311_17:16	Ascending	15	✓			✓	
16	S1A_IW_GRDH_1SDV_20150313_05:49	Descending	37	✓			✓	
17	S1A_IW_GRDH_1SDV_20150316_17:24	Ascending	88	✓			✓	
18	S1A_IW_GRDH_1SDV_20150323_17:16	Ascending	15				✓	
19	S1A_IW_GRDH_1SDV_20150325_05:49	Descending	37			✓		
20	S1A_IW_GRDH_1SDV_20150328_17:24	Ascending	88	✓				✓
21	S1A_IW_GRDH_1SDV_20150404_17:16	Ascending	15		✓		✓	✓
22	S1A_IW_GRDH_1SDV_20150416_17:16	Ascending	15			✓		
23	S1A_IW_GRDH_1SDV_20150515_17:24	Ascending	88			✓		
24	S1A_IW_GRDH_1SDV_20150522_17:16	Ascending	15			✓		
25	S1A_IW_GRDH_1SDV_20150819_17:24	Ascending	88			✓		
26	S1A_IW_GRDH_1SDV_20151006_17:24	Ascending	88		✓			
27	S1A_IW_GRDH_1SDV_20151030_17:24	Ascending	88		✓		✓	
28	S1A_IW_GRDH_1SDV_20151111_17:24	Ascending	88					✓
29	S1A_IW_GRDH_1SDV_20151120_05:49	Descending	37		✓	✓		
30	S1A_IW_GRDH_1SDV_20151130_17:16	Ascending	15	✓				
31	S1A_IW_GRDH_1SDV_20151202_05:49	Descending	37			✓	✓	✓
32	S1A_IW_GRDH_1SDV_20151212_17:16	Ascending	15					✓
33	S1A_IW_GRDH_1SDV_20151224_17:16	Ascending	15					✓
34	S1A_IW_GRDH_1SDV_20151226_05:49	Descending	37		✓			
35	S1A_IW_GRDH_1SDV_20160117_17:16	Ascending	15					✓
36	S1A_IW_GRDH_1SDV_20160119_05:49	Descending	37		✓			
37	S1A_IW_GRDH_1SDV_20160129_17:16	Ascending	15			✓		
38	S1A_IW_GRDH_1SDV_20160131_05:49	Descending	37			✓	✓	✓
39	S1A_IW_GRDH_1SDV_20160203_17:24	Ascending	88		✓			
40	S1A_IW_GRDH_1SDV_20160210_17:16	Ascending	15		✓	✓	✓	
41	S1A_IW_GRDH_1SDV_20160212_05:49	Descending	37		✓		✓	

42	S1A_IW_GRDH_1SDV_20160215_17:24	Ascending	88			✓	✓	✓
43	S1A_IW_GRDH_1SDV_20160224_05:49	Descending	37		✓		✓	
44	S1A_IW_GRDH_1SDV_20160307_05:49	Descending	37	✓	✓			✓
45	S1A_IW_GRDH_1SDV_20160319_05:49	Descending	37				✓	✓
46	S1A_IW_GRDH_1SDV_20160322_17:24	Ascending	88				✓	
47	S1A_IW_GRDH_1SDV_20160329_17:16	Ascending	15			✓		✓
48	S1A_IW_GRDH_1SDV_20160403_17:24	Ascending	88				✓	
49	S1A_IW_GRDH_1SDV_20160415_17:24	Ascending	88					✓
50	S1A_IW_GRDH_1SDV_20160808_17:16	Ascending	15	✓				
51	S1B_IW_GRDH_1SDV_20161013_17:16	Ascending	15			✓		
52	S1B_IW_GRDH_1SDV_20161130_17:16	Ascending	15	✓				
53	S1B_IW_GRDH_1SDV_20161205_17:24	Ascending	88		✓			
54	S1A_IW_GRDH_1SDV_20161206_17:16	Ascending	15			✓		
55	S1A_IW_GRDH_1SDV_20161220_05:49	Descending	37				✓	
56	S1A_IW_GRDH_1SDV_20161230_17:16	Ascending	15			✓		
57	S1B_IW_GRDH_1SDV_20170107_05:49	Descending	37			✓	✓	
58	S1A_IW_GRDH_1SDV_20170116_17:24	Ascending	88		✓		✓	
59	S1B_IW_GRDH_1SDV_20170117_17:16	Ascending	15		✓			
60	S1B_IW_GRDH_1SDV_20170119_05:49	Descending	37					✓
61	S1A_IW_GRDH_1SDV_20170123_17:16	Ascending	15			✓		
62	S1A_IW_GRDH_1SDV_20170125_05:49	Descending	37				✓	
63	S1B_IW_GRDH_1SDV_20170203_17:24	Ascending	88		✓			
64	S1B_IW_GRDH_1SDV_20170210_17:16	Ascending	15			✓		
65	S1A_IW_GRDH_1SDV_20170216_17:16	Ascending	15					✓
66	S1B_IW_GRDH_1SDV_20170222_17:16	Ascending	15	✓		✓		
67	S1B_IW_GRDH_1SDV_20170224_05:49	Descending	37		✓	✓	✓	✓
68	S1B_IW_GRDH_1SDV_20170227_17:24	Ascending	88					✓
69	S1A_IW_GRDH_1SDV_20170302_05:49	Descending	37	✓		✓		
70	S1A_IW_GRDH_1SDV_20170305_17:24	Ascending	88		✓			
71	S1B_IW_GRDH_1SDV_20170306_17:15	Ascending	15					✓
72	S1A_IW_GRDH_1SDV_20170312_17:16	Ascending	15					✓
73	S1A_IW_GRDH_1SDV_20170314_05:49	Descending	37		✓			
74	S1A_IW_GRDH_1SDV_20170317_17:24	Ascending	88				✓	
75	S1B_IW_GRDH_1SDV_20170318_17:16	Ascending	15		✓			
76	S1B_IW_GRDH_1SDV_20170320_05:49	Descending	37		✓			✓
77	S1B_IW_GRDH_1SDV_20170323_17:24	Ascending	88		✓			
78	S1A_IW_GRDH_1SDV_20170324_17:16	Ascending	15					✓
79	S1A_IW_GRDH_1SDV_20170326_05:49	Descending	37				✓	

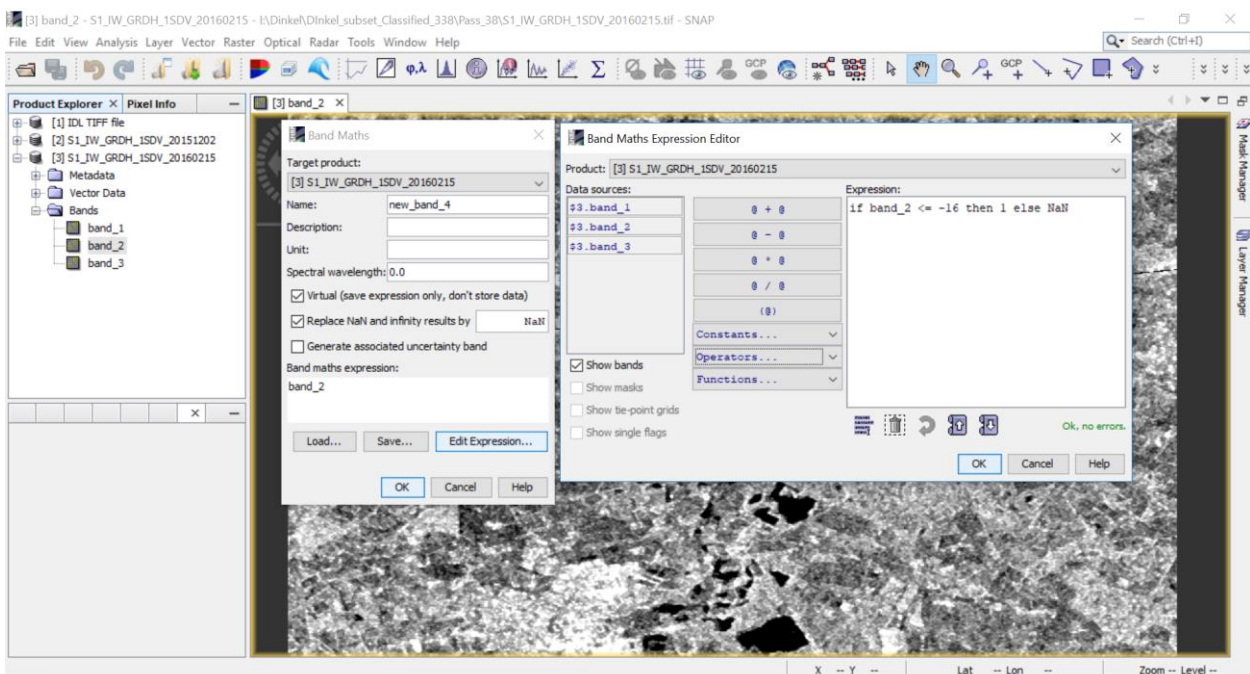
Remark: ✓ Images used for respective retention reservoir

## Appendix B: Sentinel-1 pre-processing steps

### i) SNAP batch processing graph

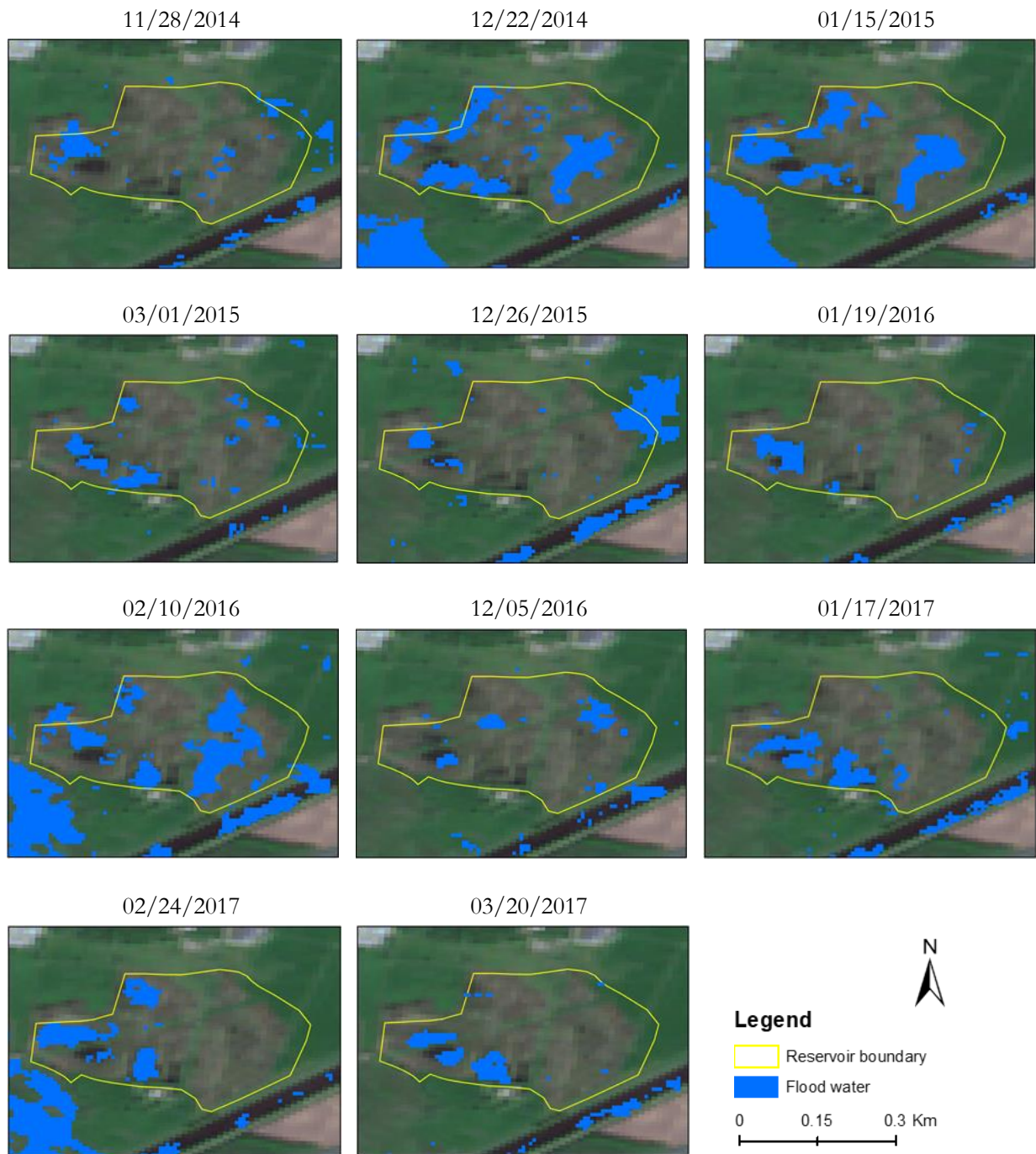


### ii) Band Maths for water pixel extraction (after pre-processing)

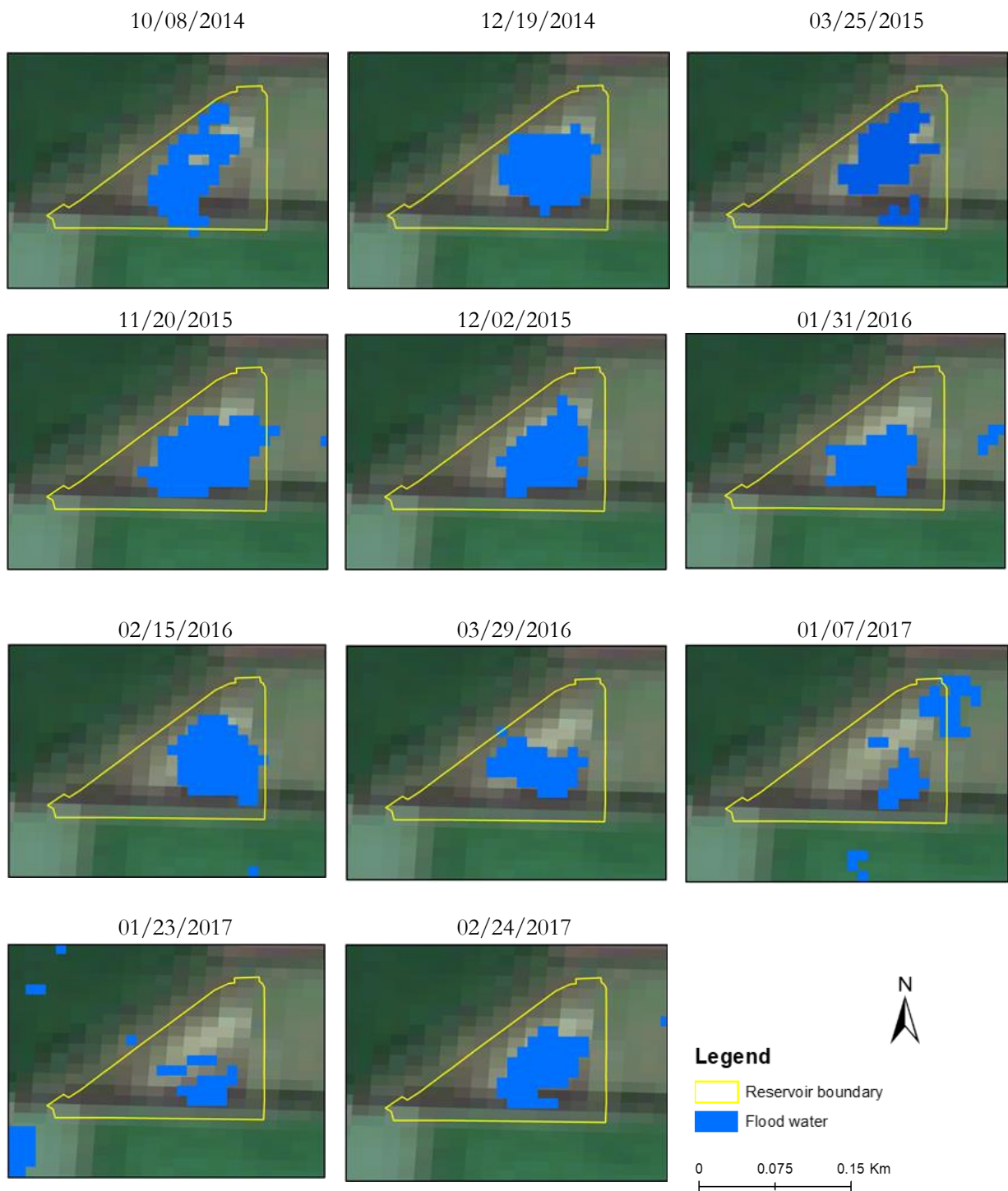


## Appendix C: Time-series flood maps for retentions reservoirs

### A) HV0001 retention reservoir



**B) OK0302 retention reservoir**



C) SZ0265 retention reservoir

---

